

Randomized Spectral Co-Clustering for Large-Scale Directed Networks

Xiao Guo

School of Mathematics

Northwest University, Xi'an, China

XIAOGUO.STAT@GMAIL.COM

Yixuan Qiu

Department of Statistics

Carnegie Mellon University, Pittsburgh, USA

YIXUANQ@GMAIL.COM

Hai Zhang

School of Mathematics

Northwest University, Xi'an, China

ZHANGHAI@NWU.EDU.CN

Xiangyu Chang*

Center of Intelligent Decision-Making and Machine Learning

School of Management

Xi'an Jiaotong University, Xi'an, China

XIANGYUCHANG@XJTU.EUD.CN

Editor:

Abstract

Directed networks are generally used to represent asymmetric relationships among units. Co-clustering aims to cluster the senders and receivers of directed networks simultaneously. In particular, the well-known spectral clustering algorithm could be modified as the spectral co-clustering to co-cluster directed networks. However, large-scale networks pose computational challenge to it. In this paper, we leverage randomized sketching techniques to accelerate the spectral co-clustering algorithms in order to co-cluster large-scale directed networks more efficiently. Specifically, we derive two series of randomized spectral co-clustering algorithms, one is *random-projection-based* and the other is *random-sampling-based*. Theoretically, we analyze the resulting algorithms under two generative models—the *stochastic co-block model* and the *degree corrected stochastic co-block model*. The approximation error rates and misclustering error rates of proposed two randomized spectral co-clustering algorithms are established, which indicate better bounds than the state-of-the-art results of co-clustering literature. Numerically, we conduct simulations to support our theoretical results and test the efficiency of the algorithms on real networks with up to tens of millions of nodes. In order to use the proposed algorithms more conveniently, a new R package called RandClust is developed and made available to the public.

Keywords: Co-clustering, Directed Network, Random Projection, Random Sampling, Stochastic co-Block Model

*. Corresponding author. The authors gratefully acknowledge the support of National Natural Science Foundation of China (NSFC, 11771012, 61502342 and U1811461)

1. Introduction

Recent advances in computing and measurement technologies have led to an explosion of large-scale network data (Newman, 2018). Networks can describe symmetric (undirected) or asymmetric (directed) relationships among interacting units in various fields, ranging from biology and informatics to social science and finance (Goldenberg et al., 2010). To extract knowledge from complex network structures, many clustering techniques, also known as community detection algorithms, are widely used to group together nodes with similar patterns (Fortunato, 2010). In particular, as asymmetric relationships are essential to the organization of networks, clustering *directed networks* is receiving more and more attentions (Chung, 2005; Boley et al., 2011; Rohe et al., 2016; Dhillon, 2001). For large-scale directed network data, an appealing clustering algorithm should have not only the statistical guarantee but also the computational advantage.

To accommodate and explore the asymmetry in directed networks, the notion of *co-clustering* was introduced in Rohe et al. (2016); Dhillon (2001), and such an idea can be traced back to Hartigan (1972). Let $A \in \{0, 1\}^{n \times n}$ be the network adjacency matrix, where $A_{ii} = 0$, and $A_{ij} = 1$ if and only if there is an edge from node i to node j . Then the i th row and column of A represent the outgoing and incoming edges for node i , respectively. Co-clustering refers to simultaneously clustering both the rows and the columns of A , so that the nodes in a row cluster share similar sending patterns, and the nodes in a column cluster share similar receiving patterns. Compared to the standard clustering where only one set of clusters is obtained, co-clustering a directed network yields two possibly different sets of clusters, which provide more insights and improve our understandings on the organization of directed networks.

Spectral clustering (Von Luxburg, 2007) is a natural and interpretable algorithm to group undirected networks, which first performs the eigen decomposition on a matrix representing the network, for example, the adjacency matrix A , and then runs k -means or other similar algorithms to cluster the resulting leading eigenvectors. Considering the asymmetry in directed networks, the standard spectral clustering algorithm has been modified to the *spectral co-clustering*, in which the eigen decomposition is replaced by the singular value decomposition (SVD), and the k -means is implemented on the left and right leading singular vectors, respectively. As the leading left and right singular vectors approximate the row and column spaces of A , it is expected that the resulting two sets of clusters contain nodes with similar sending and receiving patterns, respectively. A concrete version of the aforementioned algorithm is introduced in Rohe et al. (2016).

The spectral co-clustering is easy to be implemented and has been shown to have many nice properties (Von Luxburg, 2007; Rohe et al., 2016). However, large-scale directed networks, namely, networks with a large number of nodes or dense edges, pose great challenges to the computation of SVD. Therefore, how to improve the efficiency of spectral co-clustering while maintaining a controllable accuracy becomes an urgent need. In this paper, we consider the problem of co-clustering large-scale directed networks based on randomization techniques, a popular approach to reducing the size of data with limited information loss (Mahoney et al., 2011; Woodruff et al., 2014; Drineas and Mahoney, 2016). Randomization techniques have been widely used in machine learning to speed up fundamental problems such as the least squares regression and low rank matrix approximation

(see Drineas et al. (2006); Meng and Mahoney (2013); Nelson and Nguyen (2013); Pilanci and Wainwright (2016); Clarkson and Woodruff (2017); Halko et al. (2011); Ye et al. (2017); Martinsson (2016), among many others). The basic idea is to compromise the size of a data matrix (or tensor) by sampling a small subset of the matrix entries, or forming linear combinations of the rows or columns. The entries or linear combinations are carefully chosen to preserve the major information contained in the matrix. Hence, randomization techniques may provide a beneficial way to aiding the spectral co-clustering of large-scale directed network data.

For a network with community structure, its adjacency matrix A is low-rank in nature, so the randomization for low-rank matrix approximation can be readily used to accelerate the SVD of A (Halko et al., 2011; Martinsson, 2016; Witten and Candès, 2015). We investigate two specific strategies, namely, the random-projection-based and the random-sampling-based SVD. The random projection strategy uses some amounts of randomness to compress the original matrix A into a smaller matrix, whose rows (columns) are linear combinations of the rows (columns) of A . In this way, the dimension of A is largely reduced, and the corresponding SVD is thus sped up. As for the random sampling strategy, the starting point is that there exist fast iterative algorithms to compute the partial SVD of a sparse matrix, such as orthogonal iteration and Lanczos iteration (Baglama and Reichel, 2005; Calvetti et al., 1994), whose time complexity is generally proportional to the number of non-zero elements of A . Therefore, a good way to accelerating the SVD of A is to first sample the elements of A to obtain a sparser matrix, and then use fast iterative algorithms to compute its SVD. As a whole, the spectral co-clustering with the classical SVD therein replaced by the randomized SVD is called the randomized spectral co-clustering.

Given the fast randomization techniques, it is also critical to study the statistical accuracy of the resulting algorithms under certain generative models. To this end, we assume the directed network is generated from the *stochastic co-block model* (ScBM) or the *degree-corrected stochastic co-block model* (DC-ScBM) (Rohe et al., 2016). These two models assume the nodes are partitioned into two sets of non-overlapping blocks, one corresponding to the row cluster and the other to the column cluster. Generally, nodes in the same row (column) block are stochastic equivalent senders (receivers). That is to say, two nodes send out (receive) an edge to (from) a third node with the same probability if these two nodes are in the same row (column) cluster. The difference of these two models lies in that the degree-corrected model (Karrer and Newman, 2011; Rohe et al., 2016) considers the degree heterogeneity arising in real networks. The statistical error of the randomized spectral co-clustering is then studied under these two settings.

The main contributions of the paper are summarized as follows.

- We develop two new fast spectral co-clustering algorithms based on randomization techniques, namely, the random-projection-based and the random-sampling-based spectral co-clustering, to analyze large-scale directed networks. In particular, the proposed algorithms are applicable to networks without and with degree heterogeneity.
- We analyze the true singular vector structure of population adjacency matrices generated by the ScBM and the DC-ScBM. The results explain why the spectral co-

clustering algorithms work well for directed networks and provide insights on designing the co-clustering algorithms for networks with and without degree heterogeneity.

- We theoretically study the approximation performance and the clustering performance of the two randomization schemes under the assumption of the two block models. It turns out that under mild conditions, the approximation error rates are consistent with those in without randomization, and the misclustering error rates are better than those in Rohe et al. (2016) and Rohe et al. (2012), although the latter two are not established in the randomization scheme. This is because the technical tools that we use to bound the misclustering error are different from those in Rohe et al. (2016) and Rohe et al. (2012).
- We evaluate the randomized SVD methods on several large-scale networks with up to tens of millions of nodes. They show great efficiency and the approximate partial SVD can be computed in less than ten seconds. We also develop the corresponding R package `RandClust`¹.

The remainder of the paper is organized as follows. Section 2 introduces the randomized spectral co-clustering algorithms for co-clustering large-scale directed network. Section 3 includes the theoretical analysis of the proposed algorithms under two network models. Section 4 reviews and discusses related works. Section 5 and 6 present the experimental results of simulations and real-world data, respectively. Section 7 concludes the paper. Technical proofs are all included in the Appendix.

2. Randomized spectral co-clustering

In this section, we first review two spectral co-clustering algorithms (Rohe et al., 2012, 2016; Hartigan, 1972) for directed networks without and with degree heterogeneity, respectively. Then we use randomization techniques to derive their corresponding randomized algorithms.

As mentioned earlier, co-clustering aims to find two possibly different set of clusters, namely, co-clusters, to describe and understand the sending pattern and receiving pattern of nodes, respectively. Recall the definition of the adjacency matrix A , the i th column and i th row reveal the receiving pattern and sending pattern of node i , respectively. Hence the co-clusters are called row clusters and column clusters, respectively.

Suppose there are K^y row clusters and K^z column clusters, and without loss of generality, assume $K^y \leq K^z$. Write the partial SVD of A as $A \approx U\Sigma V$, where $U \in \mathbb{R}^{n \times K^y}$ and $V \in \mathbb{R}^{n \times K^y}$. The left singular U and the right singular vector V approximate the row space and column space of A , respectively. On the other hand, one can see that U and V are the eigenvectors of two symmetric matrices AA^\top and $A^\top A$ whose (i, j) entries correspond to the number of common children and the number of common parents of nodes i and j , respectively. Therefore, U and V contain the sending and receiving information of each node. Clustering U and V respectively would definitely yield clusters with nodes sharing similar sending and receiving patterns.

Based on the above explanations, one can see that the well-known spectral clustering is a good paradigm for co-clustering directed networks. We here consider two algorithms.

1. <https://github.com/XiaoGuo-stat/RandClust>

One is based on the standard spectral clustering. It first computes the SVD of A , and then use k -means to cluster the left and right singular vectors of A , respectively (see Algorithm 1). This algorithm is well-suited to networks whose nodes have approximately equal degree. While for networks whose nodes have heterogeneous degree, we consider the following strategy. We first compute the SVD of A , and then normalize the non-zero rows of the left and right singular vectors such that the resulting rows have Euclidean norm 1. k -median clustering is then performed on the normalized rows of the left singular vectors and the right singular vectors, respectively. After that, the zero rows of singular vectors are randomly assigned to an existing cluster (see Algorithm 2). The normalization step aims to balance the importance of each node to facilitate the subsequent clustering procedures. And as we will see in the next section, it is essential for co-clustering networks with degree heterogeneity. The k -median clustering is used partially due to its robustness to outliers, which deals with the sum of norms instead of sum of squared norms.

Algorithm 1 Spectral co-clustering with k -means

Input:

Adjacency matrix $A \in \mathbb{R}^{n \times n}$ of a directed network. Number of row clusters K^y , and number of column clusters K^z ($K^y \leq K^z$);

- 1: Compute the left singular vectors $U \in \mathbb{R}^{n \times K^y}$ and right singular vectors $V \in \mathbb{R}^{n \times K^y}$ of A .
 - 2: Run k -means on U with K^y target clusters and on V with K^z clusters.
 - 3: Output the co-clustering results.
-

Algorithm 2 Spectral co-clustering with spherical k -median

Input:

Adjacency matrix $A \in \mathbb{R}^{n \times n}$ of a directed network. Number of row clusters K^y , and number of column clusters K^z ($K^y \leq K^z$);

- 1: Compute the left singular vectors $U \in \mathbb{R}^{n \times K^y}$ and right singular vectors $V \in \mathbb{R}^{n \times K^y}$ of A .
 - 2: Let $I_+^y = \{i : \|U_{i*}\|_2 > 0\}$ and $I_+^z = \{i : \|V_{i*}\|_2 > 0\}$.
 - 3: Let U' and V' be the row-normalized version of $U_{I_+^y*}$ and $V_{I_+^z*}$, where $U_{I_+^y*}$ denotes the submatrix of U consisting of rows in I_+^y , and $V_{I_+^z*}$ can be explained similarly.
 - 4: Run k -median on U' with K^y target clusters and on V' with K^z clusters.
 - 5: The nodes outside I_+^y and I_+^z are randomly assigned to any of the estimated clusters.
 - 6: Output the clustering results.
-

Now we discuss the time complexity of Algorithm 1 and 2. It is well-known that the classical full SVD generally takes $O(n^3)$ time which is time consuming when n is large. Indeed, only the partial SVD of A is needed, which can be done by fast iterative methods. See Baglama and Reichel (2005); Calvetti et al. (1994) for example. They generally takes $O(n^2 K^y T_0)$ time, where T_0 is the iteration number corresponding to a certain error and it can be large when n is large. While for the k -means or k -median, it is well-known that finding their optimal solutions is NP-hard. Hence, efficient heuristic algorithms are commonly employed. In this paper, we use the Lloyd's algorithm to solve the k -means whose time complexity is proportional to n , and use the fast averaged stochastic gradient algorithm to solve the k -median (Cardot et al., 2013). Although these two algorithms are

not guaranteed to converge to the global solutions, we assume in the theoretical analysis that they could find the optimal solutions for simplicity. Alternatively, one can use a more delicate $(1 + \epsilon)$ -approximate k -means (Kumar et al., 2004) to bridge such gap, where a good approximate solution can be found within a constant fraction of the optimal value. Based on the above discussions, the time complexity of Algorithm 1 and 2 are dominated by the SVD, which encourages us to make use of the randomization techniques to speed up the computation of SVD for further improving the spectral co-clustering.

2.1 Random-projection-based spectral co-clustering

In this subsection we first introduce how to leverage randomized sketching techniques to accelerate SVD, and then based on that we establish the random-projection-based spectral co-clustering algorithm.

The basic idea of the random-projection-based SVD is to compress the adjacency matrix A into a smaller matrix, and then apply a standard SVD to the compressed one, thus saving the computational cost. The approximate SVD of the original A can be recovered by postprocessing the SVD of the smaller matrix (Halko et al., 2011; Martinsson, 2016; Witten and Candès, 2015).

For an asymmetric matrix A with a target rank K^y , the objective is to find orthonormal bases $Q, T \in \mathbb{R}^{n \times K^y}$ such that

$$A \approx QQ^\top ATT^\top := A^{\text{rp}}.$$

It is not hard to see that QQ^\top projects the column vectors of A to the column space of Q , and TT^\top projects the row vectors of A to the row space of T (or the column space of T^\top). Therefore, Q and T approximate the column and row spaces of A , respectively. In randomization methods, Q and T can be built via *random projection* (Halko et al., 2011). Take Q as an example, one first constructs an $n \times K^y$ random matrix whose columns are random linear combinations of the columns of A , and then orthonormalizes the K^y columns using the QR decomposition to obtain the orthonormal matrix Q . Once Q and T are constructed, we can perform the standard SVD on $Q^\top AT$, and the approximate SVD of A can be achieved by left multiplying Q and right-multiplying T . The whole procedure of the random-projection-based SVD can be summarized as the following steps:

- *Step 1:* Construct two test matrices $\Omega, \Gamma \in \mathbb{R}^{n \times K^y}$ with independent standard Gaussian entries.
- *Step 2:* Obtain Q and T via the QR decomposition $A\Omega \rightarrow QR_1$ and $A^\top\Gamma \rightarrow TR_2$.
- *Step 3:* Compute SVD of $Q^\top AT \rightarrow U_s \Sigma V_s^\top$.
- *Step 4:* Output the approximate SVD of A as $A \approx U^{\text{rp}} \Sigma (V^{\text{rp}})^\top$, where $U^{\text{rp}} := QU_s$ and $V^{\text{rp}} := TV_s$.

The *random-projection-based spectral co-clustering* refers to Algorithm 1 or 2 with the SVD therein replaced with the above random-projection-based SVD.

The *oversampling* and the *power iteration scheme* are two strategies to improve the performance of the randomized SVD (Halko et al., 2011; Martinsson, 2016). The oversampling uses extra r and s ($K^y + r$ and $K^y + s$ in total) random projections to form the sketch matrices $A\Omega$ and $A^\top\Gamma$ in *Step 2*. Such strategy reduces the information loss when the rank of A is not exactly K^y . The power iteration scheme employs $(AA^\top)^q A\Omega$ and $(A^\top A)^q A^\top\Gamma$ instead of $A\Omega$ and $A^\top\Gamma$ in *Step 2*. This treatment improves the quality of the sketch matrix when the singular values of A are not rapidly decreasing.

The time complexity of the random-projection-based SVD is dominated by the matrix multiplication operations in *Step 2* which generally takes $O((2q + 1)n^2(K^y + \max(r, s)))$ time. Note that the classical SVD in *Step 3* is cheap as the matrix dimension as low as $K^y + \max(r, s)$. Alternatively, one can implement partial SVD to find only K^y singular vectors of A . In addition, the time of *Step 2* can be further improved if one uses structured random test matrix or performs the matrix multiplication in parallel. The random-projection-based SVD is numerically stable, and it comes with good theoretical guarantee (Halko et al., 2011; Martinsson, 2016; Witten and Candès, 2015).

2.2 Random-sampling-based spectral co-clustering

In this subsection, we first introduce the accelerated SVD based on the random sampling technique and then define the corresponding spectral co-clustering algorithm.

Note that real networks are often sparse (Watts and Strogatz, 1998; Chang et al., 2019). Specifically, the number of non-zero elements in the adjacency matrix A is generally $O(n^\alpha)$ with $0 < \alpha < 2$. And we know that the time complexity of fast iterative algorithms of SVD is proportional to the number of non-zero elements of matrix (Baglama and Reichel, 2005; Calvetti et al., 1994). Thus it is efficient to find the leading singular vectors of A using iterative methods when A is really sparse. The random-sampling-based SVD is designed to make this procedure more efficient. The general idea is to first sample the elements of A randomly to obtain an random sparsified matrix of A . Then, use a fast iterative algorithm to compute the leading singular vectors of the sparsified matrix. The SVD of A can then be approximated by the partial SVD of the sparsified matrix.

We use a simple strategy to construct the sparsified matrix A^{rs} . That is, each element of A is sampled with equal probability p , and the elements that are not sampled are forced to be zero. Formally, for each pair of (i, j) ,

$$A_{ij}^{\text{rs}} = \begin{cases} \frac{A_{ij}}{p}, & \text{if } (i, j) \text{ is selected,} \\ 0, & \text{if } (i, j) \text{ is not selected.} \end{cases} \quad (3.1)$$

If the sampling probability p is not too small, then A^{rs} is close to A . With the sparsified matrix at hand, one can use fast iterative algorithms such as Baglama and Reichel (2005); Calvetti et al. (1994) to compute its leading singular vectors. We summarize the whole procedures of the random-sampling-based SVD as the following steps:

- *Step 1:* Form the sparsified matrix A^{rs} via (3.1).
- *Step 2:* Compute the partial SVD of A^{rs} using the fast iterative algorithm in Baglama and Reichel (2005) or Calvetti et al. (1994) such that $A^{\text{rs}} \approx U_{n \times K^y}^{\text{rs}} \Sigma_{K^y \times K^y} (V^{\text{rs}})_{K^y \times n}^\top$.

The *random-sampling-based spectral co-clustering* refers to Algorithm 1 or 2 with the SVD therein replaced with the above random-sampling-based SVD.

The time complexity of *Step 1* and *Step 2* are approximately $O(\|A\|_0)$ and $O(\|A^{\text{rs}}\|_0 K^y T_1)$, where $\|A\|_0$ denotes the number of non-zero elements in A , and T_1 denotes number of iterations. Generally, the number of edges in a network is far below $O(n^2)$. Hence the random-sampling-based SVD is rather efficient.

3. Theoretical analysis

In this section, we analyze the theoretical properties of the randomized spectral co-clustering algorithms under two generative models. One is the ScBM and the other is the DC-ScBM (Rohe et al., 2016).

These two models are built upon the notion of co-clustering in directed networks. Nodes are partitioned into two underlying sets of clusters. One corresponds to the row clusters and the other corresponds to the column clusters. The row and column clusters are possibly different and even have different number of clusters. Generally, nodes in a common row cluster are stochastic equivalent senders in the sense that they send out an edge to a third node with equal probabilities. Similarly, nodes in a common column cluster are stochastic equivalent receivers in the sense that they receive an edge from a third node with equal probabilities.

Before giving the formal definitions of these two models, we now provide some notes and notation. Suppose there exists K^y row clusters and K^z column clusters in the directed network $A \in \mathbb{R}^{n \times n}$. Without loss of generality, we assume throughout this paper that $K^y \leq K^z$. For $i = 1, \dots, n$, $g_i^y \in \{1, \dots, K^y\}$ and $g_i^z \in \{1, \dots, K^z\}$ denote assignments of the row cluster and column cluster of node i , respectively. We can also represent the cluster assignments using membership matrices. Let $\mathbb{M}_{n,K}$ be the set of all $n \times K$ matrices that have exactly one 1 and $K - 1$ 0's in each row. $Y \in \mathbb{M}_{n,K^y}$ is called a row membership matrix if node i belongs to row cluster g_i^y if and only if $Y_{ig_i^y} = 1$. Similarly, $Z \in \mathbb{M}_{n,K^z}$ is called a column membership matrix if node i belongs to column cluster g_i^z if and only if $Z_{ig_i^z} = 1$. For $1 \leq k \leq K^y$, let $G_k^y = \{1 \leq i \leq n : g_i^y = k\}$ be the cluster of nodes that belongs to row cluster k , and denote its size $|G_k^y| = n_k^y$. Similarly, for $1 \leq k \leq K^z$, let $G_k^z = \{1 \leq i \leq n : g_i^z = k\}$ be the cluster of nodes that belongs to column cluster k , and denote its size $|G_k^z| = n_k^z$. For any matrix B and proper index sets I and J , B_{I*} and B_{*J} denote the sub-matrices of B that consist of the rows in I and column in J , respectively. $\|B\|_F$, $\|B\|_2$, and $\|B\|_\infty$ denote the Frobenius norm, spectral norm, and the element-wise maximum absolute value of B . $\text{diag}(B)$ denotes a diagonal matrix with its diagonal entries being the same with those of B .

3.1 The stochastic co-block model

The ScBM is defined as follows,

Definition 1 (ScBM (Rohe et al., 2016)) *Let $Y \in \mathbb{M}_{n,K^y}$ and $Z \in \mathbb{M}_{n,K^z}$ be the row and column membership matrices, respectively. Let $B \in [0, 1]^{K^y \times K^z}$ be the connectivity matrix whose (k, l) th element is the probability of a directed edge from any node in the row cluster k to any node in the column cluster l . Given (Y, Z, B) , each element of the network*

adjacency matrix $A = (a_{ij})_{1 \leq i, j \leq n}$ is generated independently as $a_{ij} \sim \text{Bernoulli}(B_{g_i^y g_j^z})$ if $i \neq j$, and $a_{ij} = 0$ if $i = j$.

Define $P = YBZ^\top$ and denote its maximum and minimum non-zero singular values by σ_n and γ_n , respectively. We assume throughout this paper that $\text{rank}(P) = K^y$ and $\text{rank}(B) = K^y$. It is easy to see that P is the population version of A in the sense that $\mathbb{E}(A) = P - \text{diag}(P)$. The next lemma reveals the structure of the singular vectors in P .

Lemma 2 Consider a ScBM parameterized by $Y \in \mathbb{M}_{n, K^y}$, $Z \in \mathbb{M}_{n, K^z}$, and $B \in [0, 1]^{K^y \times K^z}$. $P = YBZ^\top$ is the population adjacency matrix with its SVD being $\bar{U}_{n \times K^y} \bar{\Sigma}_{K^y \times K^y} \bar{V}_{K^y \times n}^\top$. Then for $1 \leq i, j \leq n$,

$$(1) Y_{i*} = Y_{j*} \text{ if and only if } \bar{U}_{i*} = \bar{U}_{j*}, \text{ and for any } g_i^y \neq g_j^y, \|\bar{U}_{i*} - \bar{U}_{j*}\|_2 = \sqrt{(n_{g_i^y}^y)^{-1} + (n_{g_j^y}^y)^{-1}}.$$

(2) $Z_{i*} = Z_{j*}$ implies $\bar{V}_{i*} = \bar{V}_{j*}$. Moreover, if the columns of B are distinct, then the opposite direction holds and as a result, $Z_{i*} = Z_{j*}$ if and only if $\bar{V}_{i*} = \bar{V}_{j*}$. Further, for any $g_i^z \neq g_j^z$, $\|\bar{V}_{i*} - \bar{V}_{j*}\|_2 \geq \|B_{*g_i^z} - B_{*g_j^z}\|_2 \cdot \min_{k=1, \dots, K^y} (n_k^y)^{1/2} / \sigma_n$, where recall that σ_n is the maximum singular value of P .

Lemma 2 provides the following important facts for us. The left singular vectors \bar{U} of P reveals the true row clusters in the sense that two rows of \bar{U} are identical if and only if the corresponding nodes are in the same row cluster. And the corresponding row distance of two nodes in distinct row clusters is determined by the number of nodes in the underlying row clusters. While the story for the column clusters is slightly different. Nodes in different column clusters correspond to different rows in \bar{V} . While the opposite side does not always hold except that the columns of B are distinct. In addition, a larger column distance of B would possibly lead to a larger row distance of \bar{V} . Based on these facts, one can imagine that the spectral co-clustering algorithms 1 and 2 would estimate the true underlying clusters well if the singular vectors of A are close enough to that of P , which by the Davis-Kahan-Wedin theorem (O'Rourke et al., 2018) would hold if A and P are close in some sense.

Next, we proceed to evaluate the clustering performance of randomized spectral co-clustering algorithms. To that end, we first evaluate the deviation of the randomized adjacency matrices A^{rp} and A^{rs} from P . Then, we examine the clustering performance of randomized algorithms. We discuss the random projection and random sampling schemes, respectively.

3.1.1 RANDOM-PROJECTION-BASED SPECTRAL CO-CLUSTERING IN SCBMS

We refer to Algorithm 1 with the SVD replaced by the random-projection-based SVD. The next theorem provides the spectral deviation of A^{rp} from P .

Theorem 3 Let $A^{\text{rp}} = QQ^\top ATT^\top$ be the randomized approximation of A in the random projection scheme where the target rank is K^y , the oversampling parameters (r, s) satisfy $K^y + r \leq n$ and $K^y + s \leq n$, and the test matrices have i.i.d. standard Gaussian entries. If

$$\max_{kl} B_{kl} \leq \alpha_n \text{ for some } \alpha_n \geq c_0 \log n / n, \quad (\text{C1})$$

then for any $\epsilon > 0$, there exists a constant c_1 such that

$$\|A^{\text{rp}} - P\|_2 \leq c_1 \sqrt{n\alpha_n}, \quad (4.1)$$

with probability at least $1 - n^{-\epsilon}$.

Theorem 3 implies that the randomized adjacency matrix A^{rp} concentrates around P at the rate of $\sqrt{n\alpha_n}$ which can be regarded as the upper bound of the expected degree in the network A . The condition (C1) prevents the network from being too sparse, and it is also used in Lei and Rinaldo (2015), among others. The bound (4.1) is the same with best concentration bound of $\|A - P\|_2$ (Lei and Rinaldo, 2015; Gao et al., 2017), to the best of our knowledge. Hence in this sense, the random projection pays little price under the framework of ScBMs.

The next theorem provides an upper bound for the proportion of misclustered nodes.

Theorem 4 *Let $Y^{\text{rp}} \in \mathbb{M}_{n, K^y}$ and $Z^{\text{rp}} \in \mathbb{M}_{n, K^z}$ be the estimated membership matrices of the randomized projection-based spectral co-clustering algorithm. The other parameters are the same with those in Theorem 3. Suppose (C1) holds and recall that the maximum and minimum non-zero singular values of P are σ_n and γ_n . The following two results hold for Y^{rp} and Z^{rp} , respectively.*

(1) Define

$$\tau = \min_{l \neq k} \sqrt{(n_k^y)^{-1} + (n_l^y)^{-1}}.$$

There exists an absolute constant $c_2 > 0$ such that, if

$$\frac{K^y \alpha_n n}{n_k^y \tau^2 \gamma_n^2} \leq c_2, \quad (C2)$$

for any $k = 1, \dots, K^y$, then with probability larger than $1 - n^{-\epsilon}$ for any $\epsilon > 0$, there exists a subset $M^y \in \{1, \dots, n\}$ such that

$$\frac{|M^y|}{n} \leq c_2^{-1} \frac{K^y \alpha_n}{\tau^2 \gamma_n^2}. \quad (4.2)$$

And for $T^y = \{1, \dots, n\} \setminus M^y$, there exists a $K^y \times K^y$ permutation matrix J^y such that

$$Y_{T^y}^{\text{rp}} J^y = Y_{T^y}^*. \quad (4.3)$$

(2) Define

$$\delta = \min_{l \neq k} \|B_{*k} - B_{*l}\|_2 \cdot \min_{i=1, \dots, K^y} (n_i^y)^{1/2} / \sigma_n.$$

There exists an absolute constant $c_3 > 0$ such that, if

$$\frac{K^y \alpha_n n}{n_k^z \delta^2 \gamma_n^2} \leq c_3, \quad (C3)$$

for any $k = 1, \dots, K^z$, then with probability larger than $1 - n^{-\epsilon}$ for any $\epsilon > 0$, there exists a subset $M^z \in \{1, \dots, n\}$ such that

$$\frac{|M^z|}{n} \leq c_3^{-1} \frac{K^y \alpha_n}{\delta^2 \gamma_n^2}. \quad (4.4)$$

And for $T^z = \{1, \dots, n\} \setminus M^z$, there exists a $K^z \times K^z$ permutation matrix J^z such that

$$Z_{T^z*}^{\text{rp}} J^z = Z_{T^z*}. \quad (4.5)$$

Theorem 4 provides upper bounds for the misclustering rates with respect to row clusters and column clusters, as indicated in (4.2) and (4.4). Recalling Lemma 2, we can see that the clustering performance depends on the minimum row distances τ and δ of the population singular vectors \bar{U} and \bar{V} . As expected, larger distances imply more accurate clusters. (4.3) and (4.5) imply that nodes in T^y and T^z are correctly clustered into the underlying row clusters and column clusters up to permutations, respectively. (C2) and (C3) are technical conditions that ensure the validity of the results. They ensure that the number of misclustered nodes with respect to the row clusters and column clusters are smaller than the minimum number of the true cluster sizes n_k^y and n_k^z . That is to say, each true cluster has nodes that are correctly clustered. These conditions can be met in many cases, see Section 4 for details. In addition, when $K^y = K^z$, it can be inferred from Lemma 2 that the column clusters perform the same with row clusters. So the RHS (4.4) can be improved to that in (4.2). In the next section, we will examine the bounds in (4.2) and (4.4) and those that follow explicitly and compare them with those in Rohe et al. (2012, 2016).

3.1.2 RANDOM-SAMPLING-BASED SPECTRAL CO-CLUSTERING IN SCBMS

We refer to Algorithm 1 with the SVD replaced by the random-sampling-based SVD. The next theorem provides the deviation of A^{rs} from P in the sense of the spectral norm.

Theorem 5 *Let A^{rs} be the randomized approximation of A in the random sampling scheme where the sampling probability is p . Suppose assumption (C1) holds, then for any $\nu > 0$ and $0 < p \leq 1$, there exist constants $c_4 > 0$ and $c_5 > 0$ such that*

$$\|A^{\text{rs}} - P\|_2 \leq c_4 \max\left\{\sqrt{\frac{n\alpha_n}{p}}, \frac{\sqrt{\log n}}{p}, \Delta(n, \alpha_n, p)\right\}, \quad (4.7)$$

where

$$\Delta(n, \alpha_n, p) := \sqrt{\frac{n\alpha_n^2}{p}} \left(1 + p^{1/4} \cdot \max\left(1, \sqrt{\frac{1}{p} - 1}\right)\right),$$

with probability larger than $1 - 2n^{-\nu} - \exp\left(-c_5 np \left(1 + p^{1/4} \cdot \max\left(1, \sqrt{\frac{1}{p} - 1}\right)^2\right)\right)$.

Theorem 5 says that A^{rs} converges to P at the rate indicated in (4.7). As expected, the rate decreases as p increases. Note that (4.7) simplifies to $O(\max(\sqrt{n\alpha_n/p}, \sqrt{\log n/p}))$, provided that $p > 1/2$, which can be further reduced to $O(\sqrt{n\alpha_n/p})$ if $p > \log n/(n\alpha_n)$.

In what follows, we use $\Phi(n, p, \alpha_n)$ to denote the bound in (4.7) as,

$$\Phi(n, p, \alpha_n) := \max\left\{\sqrt{\frac{n\alpha_n}{p}}, \frac{\sqrt{\log n}}{p}, \Delta(n, \alpha_n, p)\right\}.$$

The next theorem provides an upper bound for the misclustering rates of the random-sampling-based spectral co-clustering.

Theorem 6 Let $Y^{\text{rs}} \in \mathbb{M}_{n, K^y}$ and $Z^{\text{rs}} \in \mathbb{M}_{n, K^z}$ be the estimated membership matrices of the randomized sampling-based spectral co-clustering algorithm. The other parameters are the same with those in Theorem 5. Suppose (C1) holds and recall that the minimum non-zero singular value of P is γ_n . δ and τ are defined the same with those in Theorem 4. The following two results hold for Y^{rs} and Z^{rs} , respectively.

(1) There exists an absolute constant $c_6 > 0$ such that, if

$$\frac{K^y \Phi^2(n, p, \alpha_n)}{n_k^y \tau^2 \gamma_n^2} \leq c_6, \quad (\text{C4})$$

for any $k = 1, \dots, K^y$, then with probability larger than $1 - 2n^{-\nu} - \exp\left(-c_5 np(1 + p^{1/4} \cdot \max(1, \sqrt{\frac{1}{p} - 1})^2)\right)$ for any $\nu > 0$, there exist subsets $M^y \in \{1, \dots, n\}$ such that

$$\frac{|M^y|}{n} \leq c_6^{-1} \frac{K^y \Phi^2(n, p, \alpha_n)}{n \tau^2 \gamma_n^2}. \quad (4.8)$$

And for $T^y = \{1, \dots, n\} \setminus M^y$, there exists a $K^y \times K^y$ permutation matrix J^y such that

$$Y_{T^y * }^{\text{rs}} J^y = Y_{T^y *}. \quad (4.9)$$

(2) There exists an absolute constant $c_7 > 0$ such that, if

$$\frac{K^y \Phi^2(n, p, \alpha_n)}{n_k^z \delta^2 \gamma_n^2} \leq c_7, \quad (\text{C5})$$

for any $k = 1, \dots, K^z$, then with probability larger than $1 - 2n^{-\nu} - \exp\left(-c_5 np(1 + p^{1/4} \cdot \max(1, \sqrt{\frac{1}{p} - 1})^2)\right)$ for any $\nu > 0$, there exist subsets $M^z \in \{1, \dots, n\}$ such that

$$\frac{|M^z|}{n} \leq c_7^{-1} \frac{K^y \Phi^2(n, p, \alpha_n)}{n \delta^2 \gamma_n^2}. \quad (4.10)$$

And for $T^z = \{1, \dots, n\} \setminus M^z$, there exists a $K^z \times K^z$ permutation matrix J^z such that

$$Z_{T^z * }^{\text{rs}} J^z = Z_{T^z *}. \quad (4.11)$$

The proof of Theorem 6 is similar to that of Theorem 4, hence we omit it. (4.8) and (4.10) provide upper bounds for the proportion of the misclustered nodes in the estimated row clusters and column clusters, respectively. As in the random projection scheme, the minimum non-zero row distance in the true singular vectors \bar{U} and \bar{V} , i.e., τ and δ , play an important role in the clustering performance. The clustering difficulty in the population level reveals that in the sample level. The nodes outside M^y and M^z are correctly clustered up to permutations (see (4.9) and (4.11)). (C4) and (C5) are technical conditions which ensure the validity of the results. They have the same effect with those in (C2) and (C3), and they could be achieved in many cases. In addition, the RHS (4.11) can be further improved to that in (4.9) as long as $K^y = K^z$.

3.2 The degree corrected stochastic co-block model

In the ScBM, the nodes within each row cluster and column cluster are stochastic equivalent. While in real networks, there exists hubs whose edges are far more than those of the non-hub nodes (Karrer and Newman, 2011). To model such degree heterogeneity, the DC-ScBM introduces extra parameters $\theta^y = (\theta_1^y, \theta_2^y, \dots, \theta_n^y)^\top \in \mathbb{R}_+^n$ and $\theta^z = (\theta_1^z, \theta_2^z, \dots, \theta_n^z)^\top \in \mathbb{R}_+^n$, which represent the propensity of each node to send and receive edges. The DC-ScBM is formally defined as follows,

Definition 7 (DC-ScBM (Rohe et al., 2016)) *Let $Y \in \mathbb{M}_{n, K^y}$ and $Z \in \mathbb{M}_{n, K^z}$ be the row and column membership matrices, respectively. Let $B \in [0, 1]^{K^y \times K^z}$ be the connectivity matrix whose (k, l) th element is the probability of a directed edge from any node in the row cluster k to any node in the column cluster l . Let $\theta^y \in \mathbb{R}^n$ and $\theta^z \in \mathbb{R}^n$ be the node propensity parameters. Given $(Y, Z, B, \theta^y, \theta^z)$, each element of the network adjacency matrix $A = (a_{ij})_{1 \leq i, j \leq n}$ is generated independently as $a_{ij} \sim \theta_i^y \theta_j^z \text{Bernoulli}(B_{g_i^y g_j^z})$ if $i \neq j$, and $a_{ij} = 0$ if $i = j$.*

Therefore, the probability of an edge from node i to j depends on not only the row cluster and column cluster they respectively lie in, but also the propensity of them to send and receive edges, respectively. Note that θ^y and θ^z would bring the problem of identifiability except that additional assumptions are enforced. In this paper, we assume $\max_{i \in G_k^y} \theta_i^y = 1$ and $\max_{i \in G_k^z} \theta_i^z = 1$ for each $k = 1, \dots, K^y$ and $k = 1, \dots, K^z$, respectively. Define $P = \text{diag}(\theta^y) Y B Z^\top \text{diag}(\theta^z)$, where recall that we assume $\text{rank}(P) = K^y$ and $\text{rank}(B) = K^y$, and denote the maximum and minimum of its singular values by σ_n and γ_n , respectively. P is actually the population version of A in the sense that $\mathbb{E}(A) = P - \text{diag}(P)$. Before analyzing the singular structure of P , we now introduce some notations. Let ϕ_k^y and ϕ_k^z be $n \times 1$ vectors that consistent with θ^y and θ^z respectively on G_k^y and G_k^z and zero otherwise. Thus, $\sum_{k=1}^{K^y} \phi_k^y = \theta^y$ and $\sum_{k=1}^{K^z} \phi_k^z = \theta^z$. Let $\Psi^y = \text{diag}(\|\phi_1^y\|_2, \dots, \|\phi_{K^y}^y\|_2)$, $\Psi^z = \text{diag}(\|\phi_1^z\|_2, \dots, \|\phi_{K^z}^z\|_2)$ and $\Psi^y B \Psi^z = \tilde{B}$. Define $\tilde{\theta}^y$ and $\tilde{\theta}^z$ be $n \times 1$ vectors such that the i th elements are $\theta_i^y / \|\phi_{g_i^y}^y\|_2$ and $\theta_i^z / \|\phi_{g_i^z}^z\|_2$, respectively. The next lemma shows the singular structure in P .

Lemma 8 *Consider a DC-ScBM parameterized by $Y \in \mathbb{M}_{n, K^y}$, $Z \in \mathbb{M}_{n, K^z}$, $B \in [0, 1]^{K^y \times K^z}$, $\theta^y \in \mathbb{R}^n$ and $\theta^z \in \mathbb{R}^n$. $P = \text{diag}(\theta^y) Y B Z^\top \text{diag}(\theta^z)$ is the population adjmatrix with its SVD being $\bar{U}_{n \times K^y} \bar{\Sigma}_{K^y \times K^y} \bar{V}_{K^y \times n}^\top$. Then for $1 \leq i, j \leq n$,*

(1) $\bar{U}_{i*} = \tilde{\theta}_i^y H_{k*}$ for $i \in G_k^y$, where H is an $K^y \times K^y$ orthonormal matrix. So for any $g_i^y \neq g_j^y$, $\cos(\bar{U}_{i*}, \bar{U}_{j*}) = 0$, where for any two vectors a and b , $\cos(a, b)$ is defined to be $a^\top b / \|a\|_2 \|b\|_2$.

(2) $\bar{V}_{i*} = \tilde{\theta}_i^z J_{k*}$ for $i \in G_k^z$, where J is an $K^z \times K^y$ matrix with orthonormal columns. And for any $g_i^z \neq g_j^z$, $\cos(\bar{V}_{i*}, \bar{V}_{j*}) = \cos((\tilde{B}_{*g_i^z})^\top \bar{\Sigma}^{-1}, (\tilde{B}_{*g_j^z})^\top \bar{\Sigma}^{-1})$.

The directions of two rows in \bar{U} or \bar{V} are the same if and only if the corresponding nodes lie in the same row cluster or column cluster. For example, if node i and node j are in the same row cluster k , then \bar{U}_{i*} and \bar{U}_{j*} both have direction H_{k*} . But the angles between each couple of direction tell different story for the row clusters and column clusters. For the row side, two rows of \bar{U} are perpendicular if the corresponding nodes lie in different row clusters.

While for the column side, the angle between two rows of \tilde{V} that correspond to different column clusters depends generally on the direction between the corresponding columns in a “normalized” connectivity matrix $\tilde{\Sigma}^{-1}\tilde{B}$, where \tilde{B} is defined earlier. Except these facts, Lemma 8 essentially explains why a normalization step is needed in Algorithm 2 before the k -median. It is well-known that k -median or k -means clusters nodes together if they are close in the sense of Euclidean distance. The normalization step forces any two rows of \tilde{U} or \tilde{V} to lie in the same position if the corresponding nodes are in the same row cluster or column cluster. In such way, the k -median or k -means could succeed when applied to the sample version singular vectors.

In Theorem 3 and 5, we have proved that the randomized adjacency matrices A^{rp} and A^{rs} concentrate around the population P under the ScBMs, where we actually did not make use of the explicit structure of P but only the facts that P is the population of A , and P is of rank K^y . Hence the same results hold here for the DC-ScBMs. Next, we use this results combining with Lemma 8 to analyze the misclustering performance of the randomized spectral co-clustering algorithms. We deal with the random projection and random sampling schemes, respectively.

3.2.1 RANDOM PROJECTION

We refer to Algorithm 2 with the SVD replaced by the random-projection-based SVD. The next theorem provides the misclustering rates of the random-projection-based algorithm.

Theorem 9 *Let $Y^{\text{rp}} \in \mathbb{M}_{n, K^y}$ and $Z^{\text{rp}} \in \mathbb{M}_{n, K^z}$ be the estimated membership matrices of the random-projection-based spectral co-clustering algorithm. The other parameters are the same with those in Theorem 3. Suppose (C1) holds and recall that the minimum non-zero singular value of P is γ_n . The following two results hold for Y^{rp} and Z^{rp} , respectively.*

(1) *Define*

$$\kappa_k^y := (n_k^y)^{-2} \sum_{i \in G_k^y} (\tilde{\theta}_i^y)^{-2}.$$

There exists an absolute constant $c_8 > 0$ such that, if

$$\frac{\sqrt{\sum_{k=1}^{K^y} (n_k^y)^2 \kappa_k^y} \sqrt{K^y \alpha_n n}}{\gamma_n n_k^y} \leq c_8, \quad (\text{C6})$$

for any $k = 1, \dots, K^y$, then with probability larger than $1 - n^{-\epsilon}$ for any $\epsilon > 0$ there exist subsets $M^y \in \{1, \dots, n\}$ such that

$$\frac{|M^y|}{n} \leq c_8^{-1} \frac{\sqrt{\sum_{k=1}^{K^y} (n_k^y)^2 \kappa_k^y} \sqrt{K^y \alpha_n}}{\gamma_n \sqrt{n}}. \quad (4.13)$$

And for $T^y = \{1, \dots, n\} \setminus M^y$, there exists a $K^y \times K^y$ permutation matrix J^y such that

$$Y_{T^y}^{\text{rp}} J^y = Y_{T^y}^{\text{rs}}. \quad (4.14)$$

(2) *Define*

$$\kappa_k^z := (n_k^z)^{-2} \sum_{i \in G_k^z} (\tilde{\theta}_i^z)^{-2} \|(\tilde{B}_{*k})^\top \tilde{\Sigma}^{-1}\|_2^{-2},$$

and

$$\eta(P) = \max_{g_i \neq g_j} \cos((\tilde{B}_{*g_i})^\top \bar{\Sigma}^{-1}, (\tilde{B}_{*g_j})^\top \bar{\Sigma}^{-1}).$$

There exists an absolute constant $c_9 > 0$ such that, if

$$\frac{\sqrt{\sum_{k=1}^{K^z} (n_k^z)^2 \kappa_k^z \sqrt{K^y \alpha_n n}}}{\sqrt{1 - \eta(P)} \gamma_n n_k^z} \leq c_9, \quad (\text{C7})$$

for any $k = 1, \dots, K^z$, then with probability larger than $1 - n^{-\epsilon}$ for any $\epsilon > 0$ there exist subsets $M^z \in \{1, \dots, n\}$ such that

$$\frac{|M^z|}{n} \leq c_9^{-1} \frac{\sqrt{\sum_{k=1}^{K^z} (n_k^z)^2 \kappa_k^z \sqrt{K^y \alpha_n}}}{\sqrt{1 - \eta(P)} \gamma_n \sqrt{n}}. \quad (\text{4.15})$$

And for $T^z = \{1, \dots, n\} \setminus M^z$, there exists a $K^z \times K^z$ permutation matrix J^z such that

$$Z_{T^z}^{\text{rp}} J^z = Z_{T^{z*}}. \quad (\text{4.16})$$

The quantities κ_k^y and κ_k^z can be thought of as the node heterogeneities with respect to sending and receiving edges in each cluster k , respectively. It can be shown that $\kappa_k^y \geq 1$ and the equality holds if the propensity of each node to send edges in row cluster k is homogeneous. Similarly, $\kappa_k^z \geq \|(\tilde{B}_{*k})^\top \bar{\Sigma}^{-1}\|_2^{-2}$ and the equality holds if the propensity of each node to receive edges in column cluster k is homogeneous. The quantity $\eta(P)$ represents the minimum non-zero angles among the rows of the population singular vectors \bar{V} (see the result (2) of Lemma 8), in the sense of cosine. (4.13) and (4.15) provide upper bounds for the proportion of the misclustered nodes in the estimated row clusters and column clusters, respectively. It can be seen that a larger sum of node degree heterogeneity (normalized by the number of nodes n_k^y and n_k^z) may lead to poorer misclustering performance. And different from the row clusters, the performance of the estimated column clusters also depend on $\eta(P)$. As expected, the larger the angle between the rows of population singular vectors \bar{V} , the easier the clustering procedure is. (4.14) and (4.16) indicate that nodes lying in T^y and T^z are correctly clustered into the underlying row clusters and column clusters up to the permutation. (C6) and (C7) are conditions which ensure that each true cluster has nodes that are correctly clustered. In addition, k -median is used technically in DC-ScBMs which facilitates the controlling of zero rows in the sample version singular vectors.

3.2.2 RANDOM SAMPLING

We refer to Algorithm 2 with the SVD replaced by the random-sampling-based SVD. The next theorem provides the misclustering rates of the random-sampling-based algorithm.

Theorem 10 *Let $Y^{\text{rs}} \in \mathbb{M}_{n, K^y}$ and $\hat{Z}^{\text{rs}} \in \mathbb{M}_{n, K^z}$ be the estimated membership matrices of the random-sampling-based spectral co-clustering algorithm. The other parameters are the same with those in Theorem 5. Suppose (C1) holds and recall that the minimum non-zero singular value of P is γ_n . The following two results hold for Y^{rs} and Z^{rs} , respectively. Recall that*

$$\Phi(n, p, \alpha_n) := \max \left\{ \sqrt{\frac{n \alpha_n}{p}}, \frac{\sqrt{\log n}}{p}, \Delta(n, \alpha_n, p) \right\},$$

where

$$\Delta(n, \alpha_n, p) := \sqrt{\frac{n\alpha_n^2}{p}} \left(1 + p^{1/4} \cdot \max(1, \sqrt{\frac{1}{p} - 1})\right).$$

(1) There exists an absolute constant $c_{10} > 0$ such that, if

$$\frac{\sqrt{\sum_{k=1}^{K^y} (n_k^y)^2 \kappa_k^y} \sqrt{K^y} \Phi(n, \alpha_n, p)}{\gamma_n n_k^y} \leq c_{10}, \quad (C8)$$

for any $k = 1, \dots, K^y$, then with probability larger than $1 - n^{-\epsilon}$ for any $\epsilon > 0$ there exist subsets $M^y \in \{1, \dots, n\}$ for $k = 1, \dots, K^y$ such that

$$\frac{|M^y|}{n} \leq c_{10}^{-1} \frac{\sqrt{\sum_{k=1}^{K^y} (n_k^y)^2 \kappa_k^y} \sqrt{K^y} \Phi(n, \alpha_n, p)}{\gamma_n n}. \quad (4.17)$$

And for $T^y = \{1, \dots, n\} \setminus M^y$, there exists a $K^y \times K^y$ permutation matrix J^y such that

$$Y_{T^y*}^{\text{rs}} J^y = Y_{T^y*}. \quad (4.18)$$

(2) There exists an absolute constant $c_{11} > 0$ such that, if

$$\frac{\sqrt{\sum_{k=1}^{K^z} (n_k^z)^2 \kappa_k^z} \sqrt{K^z} \Phi(n, \alpha_n, p)}{\sqrt{1 - \eta(P)} \gamma_n n_k^z} \leq c_{11}, \quad (C9)$$

for any $k = 1, \dots, K^z$, then with probability larger than $1 - n^{-\epsilon}$ for any $\epsilon > 0$ there exist subsets $M^z \in \{1, \dots, n\}$ for $k = 1, \dots, K^z$ such that

$$\frac{|M^z|}{n} \leq c_{11}^{-1} \frac{\sqrt{\sum_{k=1}^{K^z} (n_k^z)^2 \kappa_k^z} \sqrt{K^z} \Phi(n, \alpha_n, p)}{\sqrt{1 - \eta(P)} \gamma_n n}. \quad (4.19)$$

And for $T^z = \{1, \dots, n\} \setminus M^z$, there exists a $K^z \times K^z$ permutation matrix J^z such that

$$Z_{T^z*}^{\text{rs}} J^z = Z_{T^z*}. \quad (4.20)$$

We omit the proof of Theorem 10 since it is similar to that of Theorem 9. (4.17) and (4.19) gives upper bounds for the proportion of misclustered nodes with respect to the row clusters and column clusters, respectively. Similar to the results of the random projection paradigm, the clustering performance depends on the weighted sum of degree heterogeneity within each true cluster. And for the column cluster, it additionally depends on the minimum non-zero angles among the rows in the population singular vector \bar{V} . (C8), (C9), (4.18) and (4.20) have the same effect and meaning with those in Theorem 9.

4. Related work and discussion

In this section, we review and discuss the literature that is closely related to the current paper. We classify them into three groups: randomization techniques, spectral clustering, and fast SVD methods.

Randomization techniques have been used to speed up SVD algorithms; see Halko et al. (2011); Witten and Candès (2015); Martinsson (2016); Erichson et al. (2019), among others. These works analyzed the efficacy of randomization techniques for non-random matrices, whereas the novelty of this paper is that we study its theoretical properties from a statistical perspective. Specifically, we consider the adjacency matrix of a directed network generated from two typical network models, namely, the ScBM, and the DC-ScBM (Rohe et al., 2016). On the other hand, recent years have witnessed a few works studying the randomized algorithms under various statistical models, such as linear regression models, logistic regression models, and constrained regression models; see for example Ma et al. (2015); Raskutti and Mahoney (2016); Wang et al. (2019, 2017); Pilanci and Wainwright (2016); Li and Kang (2019); Zhang et al. (2020). In particular, Zhang et al. (2020) studied the randomized spectral clustering algorithms for clustering large-scale undirected networks and analyzed the theoretical properties under the framework of the stochastic block models (Holland et al., 1983). Compared with undirected networks, directed networks contain more information and bring the asymmetry that need to be accommodated. As can be seen from the theoretical results, the true row and column clusters correspond to distinct singular vector structures. Accordingly, the clustering performance of the left and right side clusters are different, and the side with a smaller target rank is easier to be properly clustered. In addition, compared with Zhang et al. (2020), we accommodate the degree heterogeneity in networks and a spherical k -median spectral co-clustering is used to co-cluster these networks. At last, we analyze the theoretical performance of the randomized version of the algorithm under the DC-ScBM.

Spectral clustering has been widely studied under different statistical models (Rohe et al., 2016, 2012; Lei and Rinaldo, 2015; Yun and Proutiere, 2016; Su et al., 2017; Qin and Rohe, 2013). In particular, Rohe et al. (2016) and its earlier version Rohe et al. (2012) are seminal works on spectral co-clustering of directed networks. They proposed the co-clustering algorithms for directed networks and studied their performance under the proposed ScBM and DC-ScBM. The differences between Rohe et al. (2016, 2012) and this work are as follows. First, they focused on the Laplacian matrix, while this paper considers the adjacency matrix that can facilitate the randomization techniques. Consequently, the technical details are quite different. Second, since the singular vectors may have zero rows, we should remove the its zero rows before the normalization step for co-clustering networks with degree heterogeneity. Therefore, we need to bound the number of removed rows in the theoretical analysis, which was not considered in Rohe et al. (2016). Third, we study the deviation of the adjacency matrices induced by the randomization techniques from the population adjacency matrix P , whereas Rohe et al. (2016) focused on the “true” Laplacian matrix. Last but not least, the misclustering bounds obtained in this paper are tighter than those in Rohe et al. (2016) and Rohe et al. (2012), although the latter two studied the non-randomized spectral co-clustering.

Below is an example to examine the misclustering bounds in Section 3 more explicitly, and we compare them with the state-of-the-art misclustering bounds in Rohe et al. (2016) and Rohe et al. (2012). Consider the following four-parameter ScBM. The underlying number of row clusters and column clusters are the same, i.e., $K^y = K^z = K$. Each cluster has a balanced size n/K . For any pair of nodes (i, j) , a directed edge from i to j is generated with probability α_n if the row cluster of i is identical to the column cluster of j , and with probability $\alpha_n(1 - \lambda)$ otherwise. Formally,

$$P = YBZ^\top = Y(\alpha_n\lambda I_K + \alpha_n(1 - \lambda)1_K1_K^\top)Z^\top.$$

It can be seen that the minimum non-zero singular value of P is $n\alpha_n\lambda/K$ (Rohe et al., 2011). Note that in such a case, Lemma 2(1) and Lemma 8(1) also hold for the column clusters Z . Therefore, without loss of generality we only examine the misclustering rate with respect to the row clusters in Theorem 4, 6, 9, and 10, respectively.

- The bound in (4.2) reduces to $O(K^2/(n\alpha_n))$ under the four-parameter ScBM. If $\alpha_n = O(\log n/n)$, then $O(K^2/(n\alpha_n))$ vanishes as n increases provided that $K = o(\sqrt{\log n})$. While in Rohe et al. (2012) (see Corollary 4.1 therein), the misclustering rate is $o(K^3\log n/\alpha_n^4)$, and $K = O(n^{1/4}/\log n)$ is required to make the results hold. In addition, in Rohe et al. (2016) (see Corollary C.1 therein), the misclustering rate is $O(K^2\log n/n)$ provided that α_n is fixed, which is not better than the $O(K^2/n)$ in our case.
- The bound in (4.8) simplifies to $O(K^2/(pn\alpha_n))$ provided that $p > \max\{\log n/(n\alpha_n), 1/2\}$. Recall condition (C1) that when n is large, $\log n/(n\alpha_n)$ is of order $O(1)$ or $o(1)$. Hence, p could be a constant. And the resulting bound is better than those in Rohe et al. (2012) and Rohe et al. (2016).
- The bound in (4.13) reduces to $O(K/\sqrt{n\alpha_n})$, which is better than those in Rohe et al. (2016) and Rohe et al. (2012) and is the square root of the resulting bound in (4.2). This is partially because we use the k -median in the DC-ScBMs instead of the k -means in the ScBMs, for which the squaring operation is not needed when bounding the misclustered nodes. Indeed, one can also use k -median in the ScBM setting, which would theoretically lead to a smaller statistical error bound. But to be more informative, we have started from the most standard k -means-based spectral clustering algorithm in the ScBMs.
- The bound in (4.18) simplifies to $O(K/\sqrt{pn\alpha_n})$ provided that $p > \max\{\log n/(n\alpha_n), 1/2\}$, which is hence tighter than those in Rohe et al. (2016) and Rohe et al. (2012) if p is a constant.

For easy reference, we summarize the misclustering error rates mentioned above in Table 1. The major reason why the randomized algorithms lead to a better clustering result than the non-randomized algorithms in Rohe et al. (2016) and Rohe et al. (2012) is that we derive the approximation bounds of $\|A^{\text{rp}} - P\|_2$ and $\|A^{\text{rs}} - P\|_2$ based on the tightest concentration bound of $\|A - P\|_2$ (Lei and Rinaldo, 2015; Chin et al., 2015), to the best of our knowledge.

Although the randomized matrix decomposition is a relatively young field, the modern computation of SVD can be traced back to 1960s, when the seminal works Golub and Kahan

Table 1: A summary of the misclustering error rates and the corresponding conditions in this work and in Rohe et al. (2016) and Rohe et al. (2012).

	Corollary C.1 in Rohe et al. (2016)	Corollary 4.1 in Rohe et al. (2012)
Bounds	$O(K^2 \log n / n)$	$o(K^3 \log n / \alpha_n^4)$
Conditions	$\alpha_n = O(1)$	$K = O(n^{1/4} / \log n)$
	Theorem 4	Theorem 6
Bounds	$O(K^2 / (n\alpha_n))$	$O(K^2 / (pn\alpha_n))$
Conditions	(C1)	(C1), $p > \max\{\log n / (n\alpha_n), 1/2\}$
	Theorem 9	Theorem 10
Bounds	$O(K / \sqrt{n\alpha_n})$	$O(K / \sqrt{pn\alpha_n})$
Conditions	(C1)	(C1), $p > \max\{\log n / (n\alpha_n), 1/2\}$

(1965); Golub and Reinsch (1970) provided the basis for the *EISPACK* and *LAPACK* routines. For computing partial SVD of matrices, iterative algorithms flourished, such as the Lanczos algorithm and its variants (Calvetti et al., 1994; Baglama and Reichel, 2005). Iterative methods are particularly suitable for structured and sparse. In Table 2, we summarize the time complexity of SVD by iterative methods and the two proposed ones in this paper, where the meaning of the notation is given in Section 2. For the random-sampling-based SVD, the rationality is straightforward: we accelerate the iterative methods by sampling the original matrix at the price of accuracy. Our main contribution is that we rigorously studied the approximation rate of the sampling-based scheme, and found that the approximation error rate is identical to those without the sampling step, provided that the sampling rate is fixed. For the random-projection-based SVD, we compare it with iterative methods from the following two aspects. Computationally, we see from Table 2 that the projection-based SVD is generally faster than iterative methods when the matrix is dense. In addition, the projection-based SVD is inherently stable and the matrix-matrix multiplications and the computations correspond to the row side and column side can be parallelized (Halko et al., 2011), which is a great advantage over iterative methods. Surprisingly, the projection-based SVD is also theoretically sound. On the surface, the projection-based SVD does not provide a better low rank approximation for the fixed matrix A than the iterative methods do, because the latter can almost exactly find the leading singular vectors of A , while the projection-based methods only approximate the singular vectors. Nonetheless, when A is a realization from a rank- K population matrix P , which is the context of this paper, projection-based methods can yield better concentration bounds. To see this, suppose the iterative methods can find K left and right leading singular vectors of A exactly. Then iterative methods approximate A by its best rank- K approximation.

Denote the approximated A by A^{it} . Then by the triangle inequality, we have

$$\begin{aligned}\|A^{\text{it}} - P\|_2 &\leq \|A^{\text{it}} - A\|_2 + \|A - P\|_2 \\ &= \sigma_{K+1} + \|A - P\|_2 \\ &\leq 2\|A - P\|_2,\end{aligned}$$

where the last inequality follows from Weyl's inequality and σ_{K+1} denotes the $(K + 1)$ th largest singular value of A . While for the projection-based methods, we have from the proof of Theorem 4 that

$$\begin{aligned}\|A^{\text{rp}} - P\|_2 &= \|QQ^{\text{T}}ATT^{\text{T}} - P\| \\ &= \|QQ^{\text{T}}(A - P)TT^{\text{T}} + QQ^{\text{T}}PTT^{\text{T}} - P\|_2 \\ &\leq \|QQ^{\text{T}}(A - P)TT^{\text{T}}\|_2 + \|QQ^{\text{T}}PTT^{\text{T}} - P\|_2 \\ &\leq \|A - P\|_2 + \|QQ^{\text{T}}PTT^{\text{T}} - P\|_2 \\ &= \|A - P\|_2.\end{aligned}$$

Hence, in the sense of the approximation error for P , the projection-based methods lead to a better result though not in terms of order.

Table 2: A summary of the time complexity of the randomized methods in this work and other methods for computing SVD.

Method	Classical SVD	Iterative methods
Time	$O(n^3)$	$O(\ A\ _0 K^y T_0)$
Method	Projection-based SVD	Sampling-based SVD
Time	$O((2q + 1)n^2(K^y + \max(r, s)))$	$O(\ A^{\text{rs}}\ _0 K^y T_1)$

5. Numerical studies

In this section, we evaluate the finite sample performance of the random-projection-based spectral co-clustering (Projection-based SC) and the random-sampling-based spectral co-clustering (Sampling-based SC), and compare them with the original spectral co-clustering (Original SC (Algorithm 1 and 2)).

In accordance with the theoretical results, we use the following two measures to examine the empirical performance of the three methods. The first is the approximation error, defined by $\|\tilde{A} - P\|_2$, where \tilde{A} can be A , A^{rp} , or A^{rs} . The second is the misclustering rate with respect to the row clusters and column clusters, defined by $\min_{J \in E_{K^y}} \frac{1}{2n} \|\tilde{Y}J - Y\|_0$ and $\min_{J \in E_{K^z}} \frac{1}{2n} \|\tilde{Z}J - Z\|_0$, respectively, where J stands for the permutation matrix, \tilde{Y} can be Y^{rp} , Y^{rs} , or the estimated row membership matrix of the Original SC, and \tilde{Z} is similarly defined. We consider the following three simulation setups:

Simulation 1 (ScBM, $K^y = K^z$): A four-parameter ScBM (B, Y, Z) , where $K^y = K^z = 3$, and B is a diagonal dominated matrix with 0.2 on the diagonal and 0.1 elsewhere.

Each row cluster has n/K^y nodes, and each column cluster has n/K^z nodes, but their cluster assignments are not necessarily the same.

Simulation 2 (ScBM, $K^y < K^z$): A ScBM (B, Y, Z) , where $2 = K^y < K^z = 3$, and each element of B is generated independently according to $B_{k,l} \sim \text{Uniform}(0.01, 0.3)$. Each row cluster has n/K^y nodes, and each column cluster has n/K^z nodes.

Simulation 3 (DC-ScBM, $K^y < K^z$): A DC-ScBM $(B, Y, Z, \theta^y, \theta^z)$, where $2 = K^y < K^z = 3$. $B_{1*} = (0.2, 0.1, 0.1)$ and $B_{2*} = (0.1, 0.2, 0.3)$. The node propensity parameters θ_i^y 's or θ_i^z 's are generated independently, taking the value of 1 with probability 0.2, and 0.2 with probability 0.8. Each row cluster has n/K^y nodes, and each column cluster has n/K^z nodes.

The other parameters in the above simulations are fixed as follows. In the random projection scheme, the oversampling parameter is 10, the power parameter is 2, and the test matrices are formulated with i.i.d. standard Gaussian entries. In the random sampling scheme, the sampling rate is 0.7. We use the R package `RSpectra` to compute the singular vector iteratively after the sampling step, and use the R package `Gmedian` (Cardot, 2020) to solve the k -median problem. Figure 1-3 display how the approximation error and misclustering error alter with the number of nodes n . The results are averaged over 50 replications.

We can make the following observations from the results. First, for the approximation error, the three methods seem to have the similar tendency as the sample size increases. In particular, the Projection-based SC and the Sampling-based SC lead to a smaller and a larger approximation error compared with that of the Original SC. Indeed, we have shown in Section 3 that $\|A^{\text{FP}} - P\|_2 \leq \|A - P\|_2$ and $\|A^{\text{rs}} - P\|_2$ has the same order with that of $\|A - P\|_2$ for fixed p , with large probability. Hence, the empirical results are consistent with the theoretical findings. Second, for the misclustering error, all three methods yield decreasing misclustering rates as n increases. The Projection-based SC and the Sampling-based SC perform just slightly worse than the Original SC, especially when n is large, which is the setting in the paper. In addition, one may find that the performance of the estimated row clusters are better than that of the column clusters in Simulation 2 and 3. This is because $K^y < K^z$ therein, and is consistent with our theoretical results.

6. Real data analysis

We empirically evaluate the randomized spectral co-clustering algorithms on real network data, considering both the clustering accuracy and the computational efficiency.

6.1 Accuracy comparison

We compare the clustering results of the projection-based SC and the sampling-based SC with that of the original SC on a statisticians citation network (Ji and Jin, 2016). This network describes the citation relationships between statisticians who published at least one paper in the four of the top statistical journals from 2003 to the first half of 2012. If author i cited at least one paper written by author j , then there is a directed edge from node i to node j . The largest component of this network results in 2,654 nodes and 21,568 edges.

To decide the target number of clusters, we evaluate the top 50 singular values of the adjacency matrix A . As indicated in Figure 4, there is an eigengap between the third and

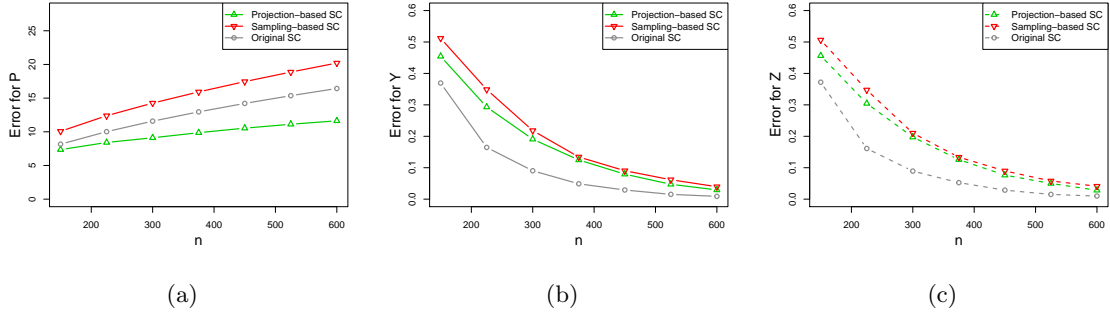


Figure 1: The results of **Simulation 1**. (a), (b), and (c) correspond to the approximation error for the population adjacency matrix P , the estimating error for the row clusters Y , and the estimating error for the column clusters Z .

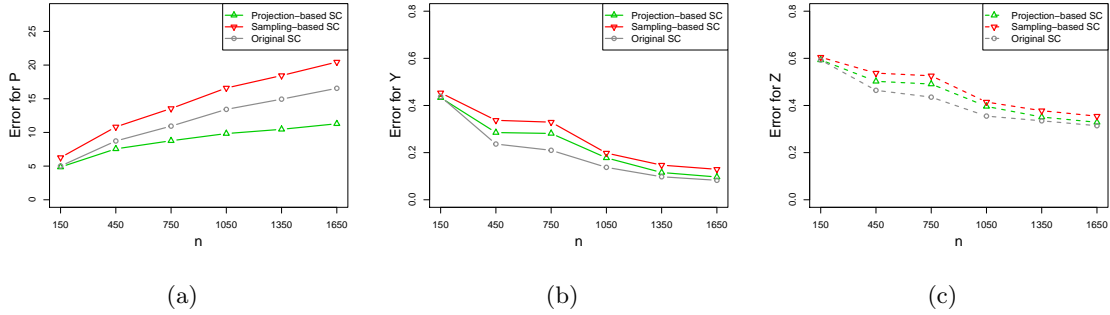


Figure 2: The results of **Simulation 2**. (a), (b), and (c) correspond to the approximation error for the population adjacency matrix P , the estimating error for the row clusters Y , and the estimating error for the column clusters Z .

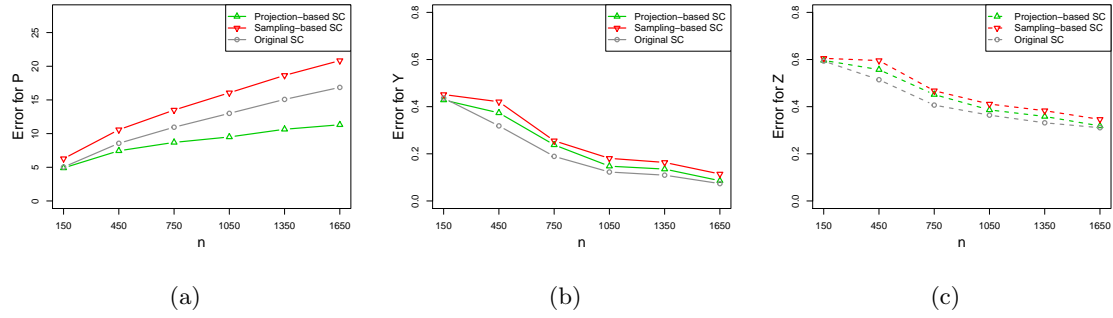


Figure 3: The results of **Simulation 3**. (a), (b), and (c) correspond to the approximation error for the population adjacency matrix P , the estimating error for the row clusters Y , and the estimating error for the column clusters Z .

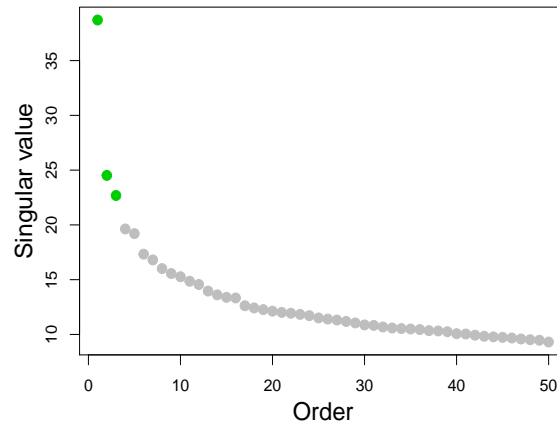


Figure 4: The top 50 singular values of the adjacency matrix of the citation network.

fourth singular values, suggesting that there are three clusters in the network. We hence set $K^y = K^z = 3$ for both sending and receiving clusters. Since hubs often appear in real networks, we use Algorithm 2 to find the clusters except that we remove the zero rows of the left and right singular vectors instead of randomly assigning a cluster to them. The parameter settings are the same with those in Section 5. Figure 5 displays the embedding of nodes provided by their corresponding components of the first three (non-normalized) singular vectors with the row (column) clusters of nodes showing in different colors. We have the following observations from Figure 5. First, the nodes corresponding to different estimated clusters lie in distinct directions, especially for the row clusters. This partially explains why the normalization step are needed for network with degree heterogeneity. Second, the row clusters and column clusters reveal different patterns. For this citation network, the authors in the same row cluster tend to have similar patterns when cited by others, and the authors in a common column cluster tend to have similar patterns when citing others. Figure 5 shows that the patterns that authors cited by others are more concentrated than the patterns that they citing others, which agrees with the common logic. Third, all three methods yield similar clusters up to certain rotations of singular vectors and clusters, which supports the theoretical findings.

6.2 Time comparison

It is well-known that the main barrier that hinders the spectral co-clustering to handle large-scale directed networks is the SVD computation. Therefore, we compare the computational time of the randomized SVD (projection-based SVD and sampling-based SVD) with the state-of-the-art approaches.

Table 3: A summary of the five real networks used in Section 6.

Data	No. of nodes	No. of edges	Target rank
Epinions social network (Richardson et al., 2003)	75,877	508,836	3
Slashdot social network (Leskovec et al., 2009)	77,360	905,468	5
Berkeley-Stanford web network (Leskovec et al., 2009)	654,782	7,499,425	4
Pokec social network (Takac and Zabovsky, 2012)	1,632,803	30,622,564	5
Wikipedia talk network (Leskovec et al., 2010)	2,388,953	5,018,445	3

Specifically, besides the proposed algorithms we also consider the classical SVD, the implicitly restarted Lanczos method (Calvetti et al., 1994), and the augmented implicitly restarted Lanczos bidiagonalization methods (Baglama and Reichel, 2005), where the last two methods are fast iterative methods for computing the leading singular vectors of large matrices and they are readily available in R package `RSpectra` Qiu and Mei (2019) and `irlba` Baglama et al. (2019), respectively. We examine five real networks with their number of nodes ranging from more than seventy thousands to more than two millions. Table 3 summarizes the basic information of each network, where the target rank means the number of singular vectors to be computed after we examine the (approximate) eigengap of the corresponding adjacency matrices.

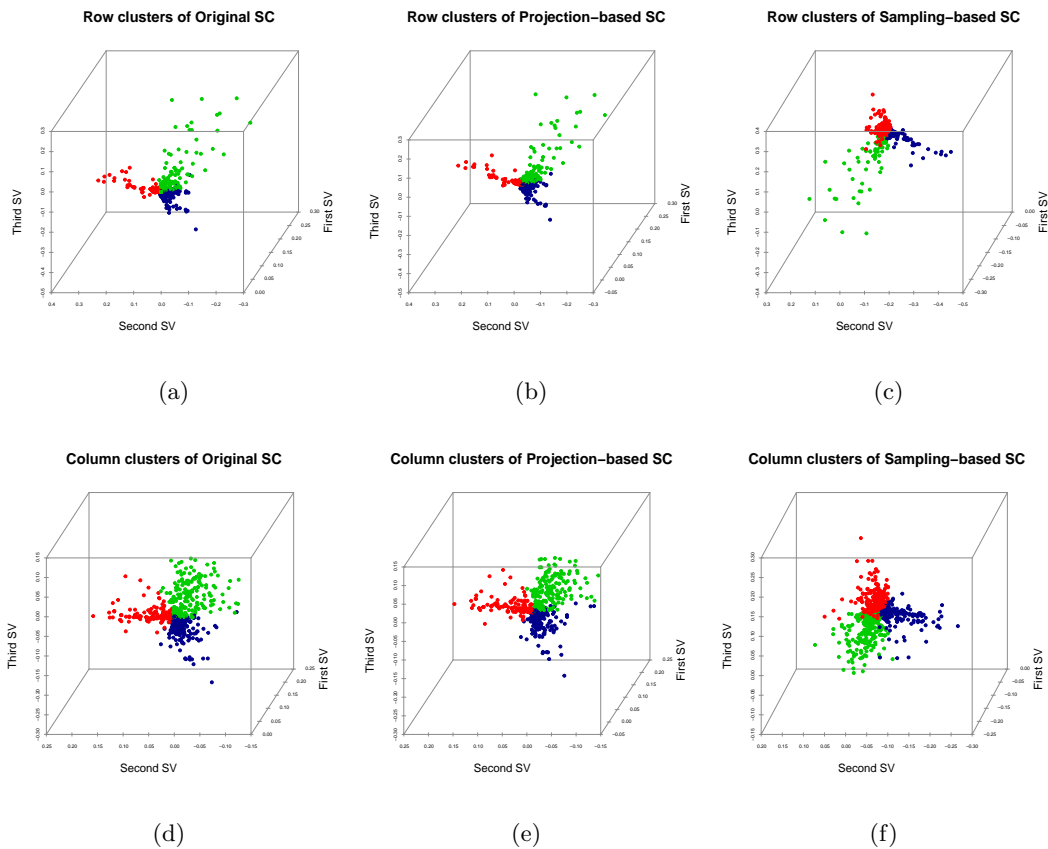


Figure 5: The embeddings of nodes provided by their corresponding components of the first three (non-normalized) singular vectors with the row (column) clusters of nodes showing in different colors. Two rows correspond to the row clustering results and the column clustering results of three methods, respectively.

Table 4: Median time (milliseconds) of each method for computing the SVD of the corresponding adjacency matrix of five real networks over 30 replications, where for the sampling-based SVD, the time with the sampling time included and excluded (shown in the parentheses) are reported, respectively.

Data	RSpectra	irlba	Projection-based	Sampling-based
Epinions social network	57.86	86.19	37.70	86.43 (79.62)
Slashdot social network	90.41	117.70	70.04	121.32 (109.17)
Berkeley-Stanford web network	816.46	781.52	482.07	817.23 (724.41)
Pokec social network	8256.82	7585.80	5645.89	6983.18 (6585.58)
Wikipedia talk network	1807.31	1467.44	1171.68	1567.58 (1489.85)

For **RSpectra** and **irlba**, the tolerance parameter is set to be 10^{-5} . For the projection-based SVD, the power parameter is 1 and the oversampling parameter is 5, which are adequate to improve the approximation quality (Halko et al., 2011). For the sampling-based SVD, the sampling parameter is 0.7, and **irlba** is used after the sampling procedure. A machine with Intel Core i7-8750H CPU 2.20GHz, 32GB memory, 64-bit Windows operating system, and R version 4.0.0 is used for all computations. Table 4 shows the median time (milliseconds) of each method for computing the SVD of the corresponding adjacency matrices of five real networks over 30 replications. For the sampling-based SVD, we report the time both including and excluding the sampling procedure.

As expected, the classical SVD failed in all five cases, and thus we did not report their time. Generally, the projection-based SVD is faster than both **RSpectra** and **irlba** in all the data sets considered. The sampling-based SVD is comparable to the baseline software packages on smaller networks, and is more advantageous on large networks, even when the sampling time is included. Based on these comparisons, we further provide evidences that the proposed randomized spectral co-clustering algorithms not only have the theoretical guarantees, but also possess the computational superiority. In conclusion, the randomization technique is a powerful tool for speeding up the classical SVD, and in real-world problems one can balance its accuracy with the time efficiency.

7. Conclusion

In this paper, we studied how randomization can be used to speed up the spectral co-clustering algorithms for co-clustering large-scale directed networks and how well the resulting algorithms perform under specific network models. In particular, the random-projection-based and random-sampling-based spectral co-clustering algorithms were derived. The clustering performance of these two algorithms were studied under the ScBM and the DC-ScBM, respectively. The theoretical bounds are high-dimensional in nature and easy to interpret. We numerically compared the randomized algorithms with fast iterative methods for computing the SVD of the adjacency matrices of real large-scale networks. It turns out that the randomized algorithms are comparable or slightly faster than the iterative methods.

In this work, we focused on the pure spectral clustering without regularization or other refinements. The current theoretical results could be further improved if one use refined spectral clustering as the starting algorithm. See Qin and Rohe (2013); Gao et al. (2017) for example. Note that the numbers of clusters were assumed to be known in the theoretical analysis. It would be important to study the selection of target cluster numbers, especially in an efficient way. In addition, it would be interesting to generalize the current framework to bipartite networks (Zhou and Amini, 2019), multi-layer networks (Lei et al., 2020), etc.

Appendix A. Proofs for ScBMs

This sections includes the proofs with respect to ScBMs.

A.1 Proof of Lemma 2

Define $\Delta_y = \text{diag}(\sqrt{n_1^y}, \dots, \sqrt{n_{K^y}^y})$ and $\Delta_z = \text{diag}(\sqrt{n_1^z}, \dots, \sqrt{n_{K^z}^z})$. Then we can write P as

$$P = YBZ^\top = Y\Delta_y^{-1}\Delta_y B\Delta_z\Delta_z^{-1}Z^\top, \quad (\text{A.1})$$

where $Y\Delta_y^{-1}$ and $Z\Delta_z^{-1}$ are both column orthogonal matrices. Denote the SVD of $\Delta_y B\Delta_z$ as $L_{K^y \times K^y} D_{K^y \times K^y} R_{K^y \times K^z}^\top$, then (A.1) implies

$$P = YBZ^\top = Y\Delta_y^{-1}LDR^\top\Delta_z^{-1}Z^\top. \quad (\text{A.2})$$

Note that L , R , $Y\Delta_y^{-1}$ and $Z\Delta_z^{-1}$ are all orthonormal matrices and recall that the SVD of P is $\bar{U}\bar{\Sigma}\bar{V}^\top$, and then we have $\bar{\Sigma} = D$,

$$\bar{U} = Y\Delta_y^{-1}L, \quad (\text{A.3})$$

and

$$\bar{V} = Z\Delta_z^{-1}R. \quad (\text{A.4})$$

For \bar{U} , since $\Delta_y^{-1}L$ is invertible, $Y_{i*} = Y_{j*}$ if and only if $\bar{U}_{i*} = \bar{U}_{j*}$. In addition, we can easily verify that the rows of $\Delta_y^{-1}L$ are perpendicular to each other and the k th row has length $\sqrt{1/n_k^y}$, therefore we have

$$\|\bar{U}_{i*} - \bar{U}_{j*}\|_2 = \sqrt{(n_{g_i^y}^y)^{-1} + (n_{g_j^y}^y)^{-1}},$$

if $g_i^y \neq g_j^y$. The argument (1) follows.

For \bar{V} , it is obvious that $Z_{i*} = Z_{j*}$ can imply $\bar{V}_{i*} = \bar{V}_{j*}$. For the opposite direction, we need additional condition on B since $\Delta_z^{-1}R$ is not invertible. In particular, we will show in the sequel that if $Z_{i*} \neq Z_{j*}$, then $\|\bar{V}_{i*} - \bar{V}_{j*}\|_2 > 0$, provided that the columns of B are distinct. To see this, suppose $Z_{iu} = 1$ and $Z_{jv} = 1$ for $1 \leq u \neq v \leq K_z$, and notice that

$$\bar{V} = Z\Delta_z^{-1}R = ZB^\top\Delta_y(L^{-1})^\top D^{-1}.$$

Then,

$$\begin{aligned} \|\bar{V}_{i*} - \bar{V}_{j*}\|_2 &= \|(Z_{i*} - Z_{j*})B^\top\Delta_y(L^{-1})^\top D^{-1}\|_2 \\ &= \|(B_{*u} - B_{*v})^\top\Delta_y(L^{-1})^\top D^{-1}\|_2, \\ &\geq \|B_{*u} - B_{*v}\|_2 \|\Delta_y(L^{-1})^\top\|_m \|D^{-1}\|_m, \end{aligned} \quad (\text{A.5})$$

where $\|M\|_m = \min_{x: \|x\|_2=1} \|Mx\|_2$. Note that $\|D^{-1}\|_m = 1/\sigma_n$ and $\|\Delta_y(L^{-1})^\top\|_m \geq \|\Delta_y\|_m \|L^{-1}\|_m = \min_{k=1, \dots, K^y} (n_k^y)^{1/2}$, where the last equality follows from the definition of Δ_y and the orthonormality of L . The argument (2) follows since $\|B_{*u} - B_{*v}\|_2 > 0$ by the assumption. \blacksquare

A.2 Proof of Theorem 3

To begin with, we notice that

$$\begin{aligned}
\|A^{\text{TP}} - P\|_2 &= \|QQ^\top ATT^\top - P\| \\
&= \|QQ^\top(A - P)TT^\top + QQ^\top PTT^\top - P\|_2 \\
&\leq \|QQ^\top(A - P)TT^\top\|_2 + \|QQ^\top PTT^\top - P\|_2 \\
&\leq \|A - P\|_2 + \|QQ^\top PTT^\top - P\|_2 \\
&=: \mathcal{I}_1 + \mathcal{I}_2,
\end{aligned} \tag{A.6}$$

where in the last inequality we used the facts that $\|AB\|_2 \leq \|A\|_2\|B\|_2$ for any matrices A and B , $\|QQ^\top\|_2 \leq 1$ and $\|TT^\top\|_2 \leq 1$. In the sequel, we discuss \mathcal{I}_1 and \mathcal{I}_2 , respectively.

To bound \mathcal{I}_1 , namely, the deviation of adjacency matrix from its population, we use the results in Lei and Rinaldo (2015). Specifically, under condition (C1), there exists a constant c_1 such that

$$\|A - P\|_2 \leq c_1 \sqrt{n\alpha_n}. \tag{A.7}$$

with probability at least $1 - n^{-\epsilon}$ for any $\epsilon > 0$, where $c_0 > 0$ is the constant in (C1).

To bound \mathcal{I}_2 , we first notice that

$$\begin{aligned}
\mathcal{I}_2 &= \|P - QQ^\top P + QQ^\top P - QQ^\top PTT^\top\|_2 \\
&\leq \|P - QQ^\top P\|_2 + \|P - PTT^\top\|_2.
\end{aligned} \tag{A.8}$$

Next we show that both terms in (A.8) are 0. We consider the first term $\|P - QQ^\top P\|_2$. We will first investigate the case without power iteration, where the sketch matrix $S^z = P\Omega^z$ and Ω^z is the $n \times (K^y + s)$ random test matrix. After that, we will turn to the power iteration scheme. Let us introduce some notation now. Partition the eigen decomposition of P as follows,

$$P = U_0 \begin{bmatrix} \Sigma_1 & \\ & 0 \end{bmatrix} \begin{bmatrix} U_1^\top \\ U_2^\top \end{bmatrix}, \tag{A.9}$$

where $U_0 \in \mathbb{R}^{n \times n}$, $U_1 \in \mathbb{R}^{n \times K^y}$, $U_2 \in \mathbb{R}^{n \times (n - K^y)}$, and $\Sigma_1 \in \mathbb{R}^{K^y \times K^y}$. Denote $\Omega_1 = U_1^\top \Omega^z$ and $\Omega_2 = U_2^\top \Omega^z$. By (A.9), the sketch matrix S^z can be written as

$$S^z = P\Omega^z = U_0 \begin{bmatrix} \Sigma_1 \Omega_1 \\ 0 \end{bmatrix}. \tag{A.10}$$

Further, define

$$\tilde{P} = U_0^\top P = \begin{bmatrix} \Sigma_1 U_1^\top \\ 0 \end{bmatrix}, \quad \tilde{S}^z = \tilde{P}\Omega^z = \begin{bmatrix} \Sigma_1 \Omega_1 \\ 0 \end{bmatrix},$$

and $\mathcal{P}_{S^z} = QQ^\top$. With these notation, we can obtain the following observations,

$$\begin{aligned}
\|P - QQ^\top P\|_2 &= \|(I - \mathcal{P}_{S^z})P\|_2 = \|U_0^\top (I - \mathcal{P}_{S^z})U_0 \tilde{P}\|_2 \\
&= \|(I - \mathcal{P}_{U_0^\top S^z})\tilde{P}\|_2 = \|(I - \mathcal{P}_{\tilde{S}^z})\tilde{P}\|_2,
\end{aligned} \tag{A.11}$$

where the second equality can be implied from the *unitary invariance* property of the spectral norm, that is, $\|UAU^\top\|_2 = \|A\|_2$ for any *unitary* (square orthonormal) matrix U ,

i.e., $UU^\top = U^\top U = I$, and the third equality follows from the following fact (Proposition 8.4 in Halko et al. (2011)) that for any unitary matrix U ,

$$U^\top \mathcal{P}_M U = \mathcal{P}_{U^\top M}. \quad (\text{A.12})$$

So, the RHS of (A.11) is 0 since

$$\text{range}(\tilde{P}) = \text{range} \begin{bmatrix} \Sigma_1 U_1^\top \\ 0 \end{bmatrix} = \text{range} \begin{bmatrix} \Sigma_1 \Omega_1 \\ 0 \end{bmatrix} = \text{range}(\tilde{S}^z), \quad (\text{A.13})$$

where we used the fact that U_1 is of full column rank and Ω_1 is of full row rank with probability 1 by recalling the assumption that the test matrix Ω^z has i.i.d. standard Gaussian entries. As a result, we have proved $\|P - QQ^\top P\|_2 = 0$ when $S^z = P\Omega^z$. When $S^z = (P^\top P)^q P\Omega^z$, by the Theorem 9.2 of Halko et al. (2011),

$$\|(I - \mathcal{P}_{S^z})P\|_2 \leq \|(I - \mathcal{P}_{S^z})(P^\top P)^q P\|_2^{1/(2q+1)} = 0, \quad (\text{A.14})$$

where the last equality follows from the fact that rank of $(P^\top P)^q P$ is not larger than K^y . Till now, we have verified the first term of \mathcal{I}_2 is 0. Similarly, we can show the second term is also 0.

Combining the bounds for \mathcal{I}_1 and \mathcal{I}_2 , the results of Theorem 3 follows. \blacksquare

A.3 Proof of Theorem 4

Generally, we will first bound the perturbation of estimated eigenvectors, and then bound the size for nodes corresponding to a large eigenvector perturbation. At last, we use Lemma 2 to show the remaining nodes are clustered properly. To fix ideas, we now recall and introduce some notation. \bar{U} and \bar{V} denote the left and right K^y leading eigenvectors of P , respectively. Accordingly, U^{rp} and V^{rp} denote the left and right K^y leading eigenvectors of A^{rp} . Likewise, $\tilde{U}^{\text{rp}} := Y^{\text{rp}} X_y^{\text{rp}}$ and $\tilde{V}^{\text{rp}} := Z^{\text{rp}} X_z^{\text{rp}}$ denote the output of the random-projection-based spectral clustering, where X_y^{rp} and X_z^{rp} denote the centroids. Next, we discuss the performance of two types of clusters, respectively.

(1) The left side. First, by the modified Davis-Kahan-Wedin sine theorem (O'Rourke et al., 2018) (See Lemma 11), there exists a $K^y \times K^y$ orthogonal matrix O such that,

$$\|U^{\text{rp}} - \bar{U}O\|_{\text{F}} \leq \frac{2\sqrt{2K^y}}{\gamma_n} \|A^{\text{rp}} - P\|_2. \quad (\text{A.15})$$

And note that

$$\begin{aligned} \|\tilde{U}^{\text{rp}} - \bar{U}O\|_{\text{F}}^2 &= \|\tilde{U}^{\text{rp}} - U^{\text{rp}} + U^{\text{rp}} - \bar{U}O\|_{\text{F}}^2 \\ &\leq \|\bar{U}O - U^{\text{rp}}\|_{\text{F}}^2 + \|U^{\text{rp}} - \bar{U}O\|_{\text{F}}^2 \\ &= 2\|U^{\text{rp}} - \bar{U}O\|_{\text{F}}^2, \end{aligned} \quad (\text{A.16})$$

where the first inequality follows because we assume that \tilde{U}^{rp} is the global solution minimum of the following k -means objective and $\bar{U}O$ is a feasible solution,

$$(Y^{\text{rp}}, X^{\text{rp}}) = \arg \min_{Y \in \mathbb{M}_n, X \in \mathbb{R}^{K^y \times K^y}} \|YX - U^{\text{rp}}\|_{\text{F}}^2.$$

So combining (A.16) with (A.15) and the bound of $\|A^{\text{rp}} - P\|_2$ in Theorem 3, we have with probability larger than $1 - n^{-\epsilon}$ that

$$\|\tilde{U}^{\text{rp}} - \bar{U}O\|_{\text{F}} \leq \frac{c_1 4\sqrt{K^y n \alpha_n}}{\gamma_n}. \quad (\text{A.17})$$

For notational convenience, we denote the RHS of (A.17) as $\text{err}(K^y, n, c_1, \alpha_n, \gamma_n)$ in what follows.

Now, we begin to bound the fraction of misclustered nodes. Recall

$$\tau = \min_{l \neq k} \sqrt{(n_k^y)^{-1} + (n_l^y)^{-1}}, \quad (\text{A.18})$$

and define

$$M^y = \{i \in \{1, \dots, n\} : \|\tilde{U}_{i*}^{\text{rp}} - (\bar{U}O)_{i*}\|_{\text{F}} > \frac{\tau}{2}\}, \quad (\text{A.19})$$

where M^y is actually the number of misclustered nodes up to permutations as we will see soon. By the definition of M^y , we can see obviously that

$$|M^y| \leq \frac{4\|\tilde{U}^{\text{rp}} - \bar{U}O\|_{\text{F}}^2}{\tau^2} \leq \frac{4 \cdot \text{err}^2(K^y, n, c_1, \alpha_n, \gamma_n)}{\tau^2}. \quad (\text{A.20})$$

Further,

$$\frac{|M^y|}{n} \leq \frac{4\|\tilde{U}^{\text{rp}} - \bar{U}O\|_{\text{F}}^2}{\tau^2 n} \leq \frac{4 \cdot \text{err}^2(K^y, n, c_1, \alpha_n, \gamma_n)}{\tau^2 n}. \quad (\text{A.21})$$

At last, we show that the nodes outside M^y are correctly clustered. First, we have $|M^y| < n_k$ for any k by condition (C2). Define $T_k^y \equiv G_k^y \setminus M^y$, where G_k^y denotes the set of nodes within the true cluster k . Then T_k^y is not an empty set. Let $T^y = \cup_{k=1}^{K^y} T_k^y$. Essentially, the rows in $(\bar{U}O)_{T^y*}$ has a one to one correspondence with those in $\tilde{U}_{T^y*}^{\text{rp}}$. On the one hand, for $i \in T_k^y$ and $j \in T_l^y$ with $l \neq k$, $\tilde{U}_{i*}^{\text{rp}} \neq \tilde{U}_{j*}^{\text{rp}}$, otherwise the following contradiction follows

$$\begin{aligned} \tau &\leq \|(\bar{U}O)_{i*} - (\bar{U}O)_{j*}\|_2 \\ &\leq \|(\bar{U}O)_{i*} - \tilde{U}_{i*}^{\text{rp}}\|_2 + \|(\bar{U}O)_{j*} - \tilde{U}_{j*}^{\text{rp}}\|_2 \\ &< \frac{\tau}{2} + \frac{\tau}{2}, \end{aligned} \quad (\text{A.24})$$

where the first and last inequality follows from the Lemma 2(1) and the definition of M_k^y in (A.19), respectively. On the other hand, for $i, j \in T_k^y$, $\tilde{U}_{i*}^{\text{rp}} = \tilde{U}_{j*}^{\text{rp}}$, because otherwise \tilde{U}_{T^y*} has more than K^y distinct rows which is contradict with the fact that the output size for the left side cluster is K^y .

As a result, we have arrived at the conclusion (1) of Theorem 4.

(2) The right side. First, follow the same lines as in (1), we have with probability larger than $1 - n^{-\epsilon}$ that

$$\|\tilde{V}^{\text{rp}} - \bar{V}O'\|_{\text{F}} \leq \frac{c_1 4\sqrt{K^y n \alpha_n}}{\gamma_n} = \text{err}(K^y, n, c_1, \alpha_n, \gamma_n), \quad (\text{A.25})$$

where O' is an orthogonal matrix. Here we want to emphasize that \bar{V} , V^{rp} , and \tilde{V}^{rp} are all $n \times K^y$, but the population cluster size and target cluster size are both K^z . This brings different performance of the right side clusters compared to that of the left side counterpart.

Now we begin to see how the fraction of misclustered nodes corresponding to the right side differs from that corresponding to left side. Denote

$$\delta = \min_{l \neq k} \|B_{*k} - B_{*l}\|_2 \cdot \min_{s=1, \dots, K^y} (n_s^y)^{1/2} / \sigma_n, \quad (\text{A.26})$$

and define

$$M^z = \{i \in \{1, \dots, n\} : \|(\tilde{V})_{i*}^{\text{rp}} - (\bar{V}O')_{i*}\|_{\text{F}} > \frac{\delta}{2}\}, \quad (\text{A.27})$$

where M^z is actually the number of misclustered nodes up to permutations as we will see soon. By the definition of M^z , it is easy to see that

$$|M^z| \leq 4 \frac{\|\tilde{V}_{i*}^{\text{rp}} - (\bar{V}O')_{i*}\|_{\text{F}}^2}{\delta^2}. \quad (\text{A.28})$$

Moreover, we have

$$\frac{|M^z|}{n} \leq 4 \frac{\|\tilde{V}_{i*}^{\text{rp}} - (\bar{V}O')_{i*}\|_{\text{F}}^2}{\delta^2 n}. \quad (\text{A.29})$$

Finally, we show that the nodes outside M_k^z are correctly clustered up to some permutations. As the left side case, we have $|M_k^z| < n_k^z$ by condition (C3). Define $T_k^z \equiv G_k^z \setminus M_k^z$. Then T_k^z is not an empty set. Let $T^z = \cup_{k=1}^{K^z} T_k^z$. Then follow the same lines as those in (1) and note the results in Lemma 2(2), we can easily show the rows in $(\bar{V}O')_{T^z*}$ has a one to one correspondence with those in $\tilde{V}_{T^z*}^{\text{rp}}$. Hence the corresponding nodes are correctly clustered.

Till now, we have proved the results in Theorem 4. ■

A.4 Proof of Theorem 5

Let G be the adjacency matrix of an Erodös-Renyi graph with each edge probability being $0 < p < 1$, then it is easy to see that $A^{\text{rs}} = \frac{1}{p}G \circ A$, where \circ denotes the entry-wise multiplication. Note that

$$\begin{aligned} \|A^{\text{rs}} - P\|_2 &= \left\| \frac{1}{p}G \circ A - P \right\|_2 \\ &= \left\| \frac{1}{p}G \circ (A - P) + \frac{1}{p}G \circ P - P \right\|_2 \\ &\leq \left\| \frac{1}{p}G \circ (A - P) \right\|_2 + \left\| \frac{1}{p}G \circ P - P \right\|_2, \\ &= \mathcal{I}_1 + \mathcal{I}_2. \end{aligned} \quad (\text{A.30})$$

In the sequel, we discuss \mathcal{I}_1 and \mathcal{I}_2 , respectively.

First, We bound \mathcal{I}_1 using Lemma 12, which provides the a spectral-norm bound of a random matrix with independent and bounded entries. In particular, we proceed by conditioning on $A - P \equiv W$. Write $(G \circ W)_{ij} = g_{ij}W_{ij}$, where $g_{ij} \sim \text{Bernoulli}(p)$. By simple calculations, we have,

$$\begin{aligned} \sigma_1 &:= \max_i \sqrt{\mathbb{E}(\sum_j g_{ij}^2 W_{ij}^2 | W)} = \max_i \sqrt{\sum_j W_{ij}^2 \mathbb{E}(g_{ij}^2 | W)} \\ &\leq \max_i \sqrt{p} \sqrt{\|W_{i*}\|_2^2} \leq \sqrt{p} \|W\|_2. \end{aligned} \quad (\text{A.31})$$

Analogously, (A.31) also holds for

$$\sigma_2 := \max_j \sqrt{\mathbb{E}(\sum_i g_{ij}^2 W_{ij}^2 | W)}.$$

With these bounds, we have by Lemma 12 that with probability $1 - n^{-\nu}$, there exists constant $c(\nu)$ such that,

$$\mathcal{I}_1 \leq \frac{1}{p} c \max(\sqrt{p} \|W\|_2, \sqrt{\log n}). \quad (\text{A.32})$$

Further, by the concentration bound $\|A - P\|_2$ in Lei and Rinaldo (2015), we have by condition (C1) that,

$$\|W\|_2 = \|A - P\|_2 \leq c' \sqrt{n\alpha_n}, \quad (\text{A.33})$$

with probability larger than $1 - n^{-\nu}$. Note that we use c, c', c'' to represent the generic constants and they may be different from line to line. Combining (A.33) with (A.32), we have with probability larger than $1 - 2n^{-\nu}$ that,

$$\mathcal{I}_1 \leq c'' \max\left(\sqrt{\frac{n\alpha_n}{p}}, \frac{\sqrt{\log n}}{p}\right). \quad (\text{A.34})$$

Second, we bound \mathcal{I}_2 . We will use Lemma 13 which provides bounds on the spectral deviation of a random matrix from its expectation. Specifically, B and X in Lemma correspond to P and $\frac{1}{p}G \circ P$ in our case. It is easy to see that $\mathbb{E}(X) = B$ and $\max_{jk} |X_{jk}| \leq \alpha_n/p$. Moreover, we have

$$\text{Var} X_{jk} \leq P_{jk}^2/p,$$

and

$$\begin{aligned} \mathbb{E}(X_{jk} - P_{jk})^4 &\leq \text{Var} X_{jk} \cdot \|X_{jk} - P_{jk}\|_\infty^2 \\ &\leq \frac{P_{jk}^2}{p} \cdot \max\left(P_{jk}, \frac{P_{jk}}{p} - P_{jk}\right)^2 \\ &= \frac{P_{jk}^4}{p} \cdot \max\left(1, \left(\frac{1}{p} - 1\right)\right)^2. \end{aligned} \quad (\text{A.35})$$

Therefore, by Lemma 13 and the fact that $P_{ij} \leq \alpha_n$, we have

$$\begin{aligned} \mathcal{I}_2 &\leq c \left(2\alpha_n \sqrt{\frac{n}{p}} + \alpha_n \frac{\sqrt{n}}{p^{1/4}} \max\left(1, \sqrt{\frac{1}{p} - 1}\right) \right) \\ &\leq c' \sqrt{\frac{n\alpha_n^2}{p}} \left(1 + p^{1/4} \cdot \max\left(1, \sqrt{\frac{1}{p} - 1}\right) \right), \end{aligned} \quad (\text{A.36})$$

with probability larger than $1 - \exp\left(-c'' np(1 + p^{1/4} \cdot \max(1, \sqrt{\frac{1}{p} - 1})^2)\right)$.

Finally, combining (A.36) with (A.34), we will obtain the conclusion in Theorem 5. \blacksquare

Appendix B. Proofs for DC-ScBMs

This section includes the proofs with respect to DC-ScBMs.

B.1 Proof of Lemma 8

Define \tilde{Y} and \tilde{Z} be normalized membership matrices such that $\tilde{Y}(i, k) = \tilde{\theta}_i^y$ if $i \in G_k^y$ and $\tilde{Y}(i, k) = 0$ otherwise, and accordingly $\tilde{Z}(i, k) = \tilde{\theta}_i^z$ if $i \in G_k^z$ and $\tilde{Z}(i, k) = 0$ otherwise. Then it is easy to see $\tilde{Y}^\top \tilde{Y} = I$ and $\tilde{Z}^\top \tilde{Z} = I$. Let $\Psi^y = \text{diag}(\|\phi_1^y\|_2, \dots, \|\phi_{K^y}^y\|_2)$ and $\Psi^z = \text{diag}(\|\phi_1^z\|_2, \dots, \|\phi_{K^z}^z\|_2)$. Then after some rearrangements, we can see that

$$\text{diag}(\theta^y)Y = \tilde{Y}\Psi^y, \quad \text{diag}(\theta^z)Z = \tilde{Z}\Psi^z. \quad (\text{B.1})$$

Thus,

$$P = \text{diag}(\theta^y)YBZ^\top \text{diag}(\theta^z) = \tilde{Y}\Psi^yB\Psi^z\tilde{Z}^\top. \quad (\text{B.2})$$

Denote the SVD of $\Psi^yB\Psi^z$ as

$$\Psi^yB\Psi^z = H_{K^y \times K^y} D_{K^y \times K^y} J_{K^y \times K^z}, \quad (\text{B.3})$$

where H and J have orthonormal columns. Then, (B.2) implies

$$P = \tilde{Y}H D J^\top \tilde{Z}^\top. \quad (\text{B.4})$$

By the orthonormality of \tilde{Y}, \tilde{Z}, H and J , we have

$$\bar{U} = \tilde{Y}H, \quad \bar{V} = \tilde{Z}J, \quad \bar{\Sigma} = D.$$

Specifically, $\bar{U}_{i*} = \tilde{\theta}_i^y H_{k*}$ for $i \in G_k^y$, and $\bar{V}_{i*} = \tilde{\theta}_i^z J_{k*}$ for $i \in G_k^z$. Since H is square matrix with orthonormal columns, $\cos(\bar{U}_{i*}, \bar{U}_{j*}) = 0$ if $g_i^y \neq g_j^y$. Thus the argument (1) follows.

Now we proceed to calculate $\cos(\bar{V}_{i*}, \bar{V}_{j*})$ for $g_i^z \neq g_j^z$. Without loss of generality, we assume $g_i^z = k, g_j^z = l$. First notice that,

$$\cos(\bar{V}_{i*}, \bar{V}_{j*}) = \frac{\bar{V}_{i*} \bar{V}_{j*}^\top}{\|\bar{V}_{i*}\|_2 \|\bar{V}_{j*}\|_2} = \frac{\tilde{\theta}_i^z \tilde{\theta}_j^z J_{k*} J_{l*}^\top}{\tilde{\theta}_i^z \tilde{\theta}_j^z \|J_{k*}\|_2 \|J_{l*}\|_2}, \quad (\text{B.5})$$

where we note that \bar{V}_{i*} and \bar{V}_{j*} are row vectors. We will discuss the numerator and denominator of (B.5), respectively. By (B.3), we have

$$J = \Psi^z B^\top \Psi^y D^{-1} (H^{-1})^\top := \tilde{B}^\top D^{-1} (H^{-1})^\top, \quad (\text{B.6})$$

where we define $\Psi^y B \Psi^z := \tilde{B}$. Therefore, we have

$$|J_{k*} J_{l*}^\top| = |\tilde{B}_{*k}^\top D^{-1} (H^{-1})^\top H^\top D^{-1} \tilde{B}_{*l}| = |\tilde{B}_{*k}^\top D^{-2} \tilde{B}_{*l}|. \quad (\text{B.7})$$

And we have

$$\|J_{k*}\|_2 = \|\tilde{B}_{*k}^\top D^{-1} (H^{-1})^\top\|_2 = \|\tilde{B}_{*k}^\top D^{-1}\|_2, \quad (\text{B.8})$$

which follows from the orthogonality of H . Similarly, $\|J_{l*}\|_2 = \|\tilde{B}_{*l}^\top D^{-1}\|_2$. Combining (B.7) and (B.8) with (B.5), we have

$$\cos(\bar{V}_{i*}, \bar{V}_{j*}) = \cos(\tilde{B}_{*g_i}^\top \bar{\Sigma}^{-1}, \tilde{B}_{*g_j}^\top \bar{\Sigma}^{-1}).$$

Thus the argument (2) holds.

B.2 Proof of Theorem 9

To fix ideas, we now recall and introduce some notation. \bar{U} and \bar{V} denote the left and right K^y leading eigenvectors of P , respectively. Accordingly, U^{rp} and V^{rp} denote the left and right K^y leading eigenvectors of A^{rp} . Note that the rows of \bar{U} and \bar{V} are all non-zero, but the rows of U^{rp} and V^{rp} might be zero. Define $I_+^y = \{i, U_{i*}^{\text{rp}} \neq 0\}$ and $I_+^z = \{i, V_{i*}^{\text{rp}} \neq 0\}$ be the index sets of non-zero rows in U^{rp} and V^{rp} . Accordingly, let $I_0^y = (I_+^y)^c$ and $I_0^z = (I_+^z)^c$. Define $(U^{\text{rp}})'$ and $(V^{\text{rp}})'$ be the row-normalized version of U^{rp} and V^{rp} with their non-zero rows removed. Define \bar{U}^{no} and \bar{V}^{no} be the row-normalized version of \bar{U} and \bar{V} . Let $\bar{U}' = \bar{U}_{I_+^{no}}^{no}$ and $\bar{V}' = \bar{V}_{I_+^{no}}^{no}$ be the sub-matrices of \bar{U}^{no} and \bar{V}^{no} that consist of the non-zero rows in U^{rp} and V^{rp} . $\tilde{U}^{\text{rp}} := Y^{\text{rp}}X_y^{\text{rp}}$ and $\tilde{V}^{\text{rp}} := Z^{\text{rp}}X_z^{\text{rp}}$ denote the output of the randomized spectral clustering (Algorithm). $(\tilde{U}^{\text{rp}})'$ and $(\tilde{V}^{\text{rp}})'$ denote the sub-matrices of \tilde{U}^{rp} and \tilde{V}^{rp} that consist of non-zero rows in U^{rp} and V^{rp} . Note that we generally use primes to represent the corresponding submatrix with zero rows in $I_0^y = (I_+^y)^c$ and $I_0^z = (I_+^z)^c$ being removed.

Generally, we will first bound the eigenvector perturbation of $U^{\text{rp}}(V^{\text{rp}})$ from $\bar{U}(\bar{V})$. Then, we bound the size of $I_0^y(I_0^z)$, namely, the number of zero rows in $U^{\text{rp}}(V^{\text{rp}})$. After that, we bound the eigenvector perturbation of $(\tilde{U}^{\text{rp}})'((\tilde{V}^{\text{rp}})')$ from $\bar{U}'(\bar{V}')$. At last, we bound the size of misclustered nodes and complete the proof. In the sequel, we discuss the performance of two types of clusters, respectively.

(1) The left side. First, by the modified Davis-Kahan-Wedin sine theorem (Theorem 19 in O'Rourke et al. (2018)), there exists a $K^y \times K^y$ orthogonal matrix O such that,

$$\|U^{\text{rp}} - \bar{U}O\|_{\text{F}} \leq \frac{2\sqrt{2K^y}}{\gamma_n} \|A^{\text{rp}} - P\|_2. \quad (\text{B.9})$$

Combining (B.9) with the results in Theorem 3, we have

$$\|U^{\text{rp}} - \bar{U}O\|_{\text{F}} \leq c \frac{2\sqrt{2K^y}}{\gamma_n} \sqrt{n\alpha_n}, \quad (\text{B.10})$$

with probability $1 - n^{-\epsilon}$ for any $\epsilon > 0$ and some constant $c > 0$. Note that the constant c may be different from line to line in this proof. And without loss of generality, we will assume the orthogonal matrix O is the identity matrix I in the following proof.

Then, we bound I_0^y . By Cauchy-Schwarz's inequality, we have

$$\begin{aligned} \|U^{\text{rp}} - \bar{U}\|_{\text{F}}^2 &\geq \sum_{i=1}^n \mathbf{1}(U_{i*}^{\text{rp}} = 0) \|\bar{U}_{i*}\|_2^2 \\ &\geq \frac{(\sum_{i=1}^n \mathbf{1}(U_{i*}^{\text{rp}} = 0))^2}{\sum_{i=1}^n \|\bar{U}_{i*}\|_2^{-2}} = \frac{|I_0^y|^2}{\sum_{i=1}^n \|\bar{U}_{i*}\|_2^{-2}}. \end{aligned} \quad (\text{B.11})$$

So,

$$|I_0^y| \leq \sqrt{\sum_{i=1}^n \|\bar{U}_{i*}\|_2^{-2}} \|U^{\text{rp}} - \bar{U}\|_{\text{F}} \leq c \sqrt{\sum_{k=1}^{K^y} (n_k^y)^2 \kappa_k^y \frac{\sqrt{K^y n \alpha_n}}{\gamma_n}} := \bar{h}, \quad (\text{B.12})$$

where the last inequality follows from (B.10) and the definition of κ_k^y .

Now, we bound $\|(\tilde{U}^{\text{rp}})' - \bar{U}'\|_{2,1}$. Note that

$$\begin{aligned} \|(\tilde{U}^{\text{rp}})' - \bar{U}'\|_{2,1} &\leq \|(\tilde{U}^{\text{rp}})' - (U^{\text{rp}})'\|_{2,1} + \|(U^{\text{rp}})' - \bar{U}'\|_{2,1} \\ &\leq 2\|(U^{\text{rp}})' - \bar{U}'\|_{2,1}, \end{aligned} \quad (\text{B.13})$$

where the last inequality follows because we assume that $(\tilde{U}^{\text{rp}})'$ is the global solution minimum of the following k -median objective and \bar{U}' is a feasible solution,

$$((Y^{\text{rp}})', (X^{\text{rp}})') = \arg \min_{Y \in \mathbb{M}_{n-|I_0^y|, K^y}, X \in \mathbb{R}^{K^y \times K^y}} \|YX - (U^{\text{rp}})'\|_{2,1}.$$

Further, we have

$$\begin{aligned} \|(U^{\text{rp}})' - \bar{U}'\|_{2,1} &\leq 2 \sum_{i=1}^n \frac{\|U_{i*}^{\text{rp}} - \bar{U}_{i*}\|_2}{\|\bar{U}_{i*}\|_2} \\ &\leq 2 \sqrt{\sum_{i=1}^n \|U_{i*}^{\text{rp}} - \bar{U}_{i*}\|_2^2 \sum_{i=1}^n \|\bar{U}_{i*}\|_2^{-2}} \\ &\leq 2 \sqrt{\sum_{i=1}^n \|\bar{U}_{i*}\|_2^{-2} \|U^{\text{rp}} - \bar{U}\|_{\text{F}}^2} = 2\bar{h}, \end{aligned} \quad (\text{B.14})$$

where the first inequality follows from the fact that

$$\left\| \frac{a}{\|a\|_2} - \frac{b}{\|b\|_2} \right\|_2 \leq 2 \frac{\|a - b\|_2}{\max(\|a\|_2, \|b\|_2)},$$

for any vectors a and b . Combining (B.14) with (B.13), we have

$$\|(\tilde{U}^{\text{rp}})' - \bar{U}'\|_{2,1} \leq 4\bar{h}. \quad (\text{B.15})$$

Next, we bound the number of misclustered nodes. Define

$$S^y = \{i \in I_+^y : \|(\tilde{U}^{\text{rp}})_{i*} - \bar{U}_{i*}^{no}\|_2 \geq \frac{1}{\sqrt{2}}\}. \quad (\text{B.16})$$

By the definition of S^y and (B.15), we have

$$|S^y| \leq \sqrt{2} \|(\tilde{U}^{\text{rp}})' - \bar{U}'\|_{2,1} \leq 4\sqrt{2}\bar{h}. \quad (\text{B.17})$$

Combining this with (B.12), we have

$$\frac{|M^y|}{n} := \frac{|S^y| + |I_0^y|}{n} \leq (4\sqrt{2} + 1) \frac{\bar{h}}{n}. \quad (\text{B.18})$$

By condition (C6), we know that $|M^y| < n_k^y$ for all k . Hence the nodes outside those indexed by M^y but within each true cluster are not empty. That is, $G_k^y \cap (\{1, \dots, n\} \setminus M^y) \neq \emptyset$, where G_k^y denotes the set of nodes within the true cluster k . Now we show that these nodes are

clustered correctly. On the one hand, suppose $i, j \in \{1, \dots, n\} \setminus M^y$ are in different clusters, then their estimated clusters are also different. Otherwise we have

$$\begin{aligned} \|\bar{U}_{i^*}^{no} - \bar{U}_{j^*}^{no}\|_2 &\leq \|\bar{U}_{i^*}^{no} - (\tilde{U}^{\text{rp}})_{i^*}\|_2 + \|(\tilde{U}^{\text{rp}})_{j^*} - \bar{U}_{j^*}^{no}\|_2 \\ &< \sqrt{2}, \end{aligned} \quad (\text{B.19})$$

where the last inequality follows from the definition of S^y . Since $\bar{U}_{i^*}^{no}$ and $\bar{U}_{j^*}^{no}$ are normalized vectors and by Lemma 8 we know that they are orthogonal with each other, the LHS of (B.19) is $\sqrt{2}$, which contradicts with the RHS of (B.19). On the other hand, if $i, j \in \{1, \dots, n\} \setminus M^y$ are in the same cluster, then their estimated clusters are also identical. Otherwise \tilde{U}^{rp} has more than K^y distinct rows, which violates the fact that the output cluster size is K^y .

As a result, we have arrived the conclusion in (1).

(2) The right side. Following the same proof strategy with that in (1), we can show that

$$\|V^{\text{rp}} - \bar{V}\|_{\text{F}} \leq c \frac{2\sqrt{2}K^y}{\gamma_n} \sqrt{n\alpha_n}, \quad (\text{B.20})$$

and

$$|I_0^z| \leq \sqrt{\sum_{i=1}^n \|\bar{V}_{i^*}\|_2^{-2}} \|V^{\text{rp}} - \bar{V}\|_{\text{F}} \leq c \sqrt{\sum_{k=1}^{K^z} (n_k^z)^2 \kappa_k^z} \frac{\sqrt{K^y n \alpha_n}}{\gamma_n} := \bar{l}, \quad (\text{B.21})$$

where the last inequality follows from the fact that $\bar{V}_{i^*} = \tilde{\theta}_i^z \tilde{B}_{*gi}^{\text{T}} D^{-1}$ and the definition of κ_k^z . In addition, similar to the arguments in (1), we can show that

$$\|(\tilde{V}^{\text{rp}})' - \bar{V}'\|_{2,1} \leq 4\bar{l}. \quad (\text{B.22})$$

Next, we bound the number of misclustered nodes. Define

$$S^z = \{i \in I_+^z : \|(\tilde{V}^{\text{rp}})_{i^*} - \bar{V}_{i^*}^{no}\|_2 \geq \frac{\sqrt{1 - \eta(P)}}{\sqrt{2}}\}. \quad (\text{B.23})$$

By the definition of S^z ,

$$\frac{|M^z|}{n} := \frac{|S^z| + |I_0^z|}{n} \leq \left(\frac{4\sqrt{2}}{\sqrt{1 - \eta(P)}} + 1 \right) \frac{\bar{l}}{n} \leq \frac{c\bar{l}}{\sqrt{1 - \eta(P)}n}. \quad (\text{B.24})$$

By condition (C7), we know that $|M^z| < n_k^z$ for all k . Hence the nodes outside those indexed by M^z but within each true cluster are not empty. That is, $G_k^z \cap (\{1, \dots, n\} \setminus M^z) \neq \emptyset$, where G_k^z denotes the set of nodes within the true cluster k . Now we show that these nodes are clustered correctly. On the one hand, if $i, j \in \{1, \dots, n\} \setminus M^z$ are in different clusters, then their estimated clusters are also different. Otherwise we have

$$\begin{aligned} \|\bar{V}_{i^*}^{no} - \bar{V}_{j^*}^{no}\|_2 &\leq \|\bar{V}_{i^*}^{no} - (\tilde{V}^{\text{rp}})_{i^*}\|_2 + \|(\tilde{V}^{\text{rp}})_{j^*} - \bar{V}_{j^*}^{no}\|_2 \\ &< \sqrt{2(1 - \eta(P))}, \end{aligned} \quad (\text{B.25})$$

where the last inequality follows from the definition of S^z . Since $\bar{V}_{i^*}^{no}$ and $\bar{V}_{j^*}^{no}$ are normalized vectors and by Lemma 8 and the definition of $\eta(P)$, we have

$$\|\bar{V}_{i^*}^{no} - \bar{V}_{j^*}^{no}\|_2 = \sqrt{1 + 1 - 2\cos(\bar{V}_{i^*}^{no}, \bar{V}_{j^*}^{no})} \geq \sqrt{2(1 - \eta(P))}, \quad (\text{B.26})$$

which contradicts with the RHS of (B.25). On the other hand, if $i, j \in \{1, \dots, n\} \setminus M^z$ are in the same cluster, then their estimated clusters are the also identical. Otherwise \hat{V}^{TP} has more than K^z distinct rows, which contradicts the fact that the output cluster size is K^z .

As a result, we have arrived the conclusion in (2). \blacksquare

Appendix C. Auxiliary lemmas

This section includes the auxiliary lemmas that are used for proving the theorems in the paper.

Lemma 11 (Theorem 19 in O’Rourke et al. (2018)) *Consider two matrices B and C with the same dimensions. Suppose matrix B has rank $r(B)$, and denote the j th largest singular value of B as $\sigma_j(B)$. For integer $1 \leq j \leq r(B)$, suppose matrix V and V' consist of the first j singular vectors of B and C , respectively. Then*

$$\sin(V, V') \leq 2 \frac{\|B - C\|_2}{\sigma_j(B) - \sigma_{j+1}(B)},$$

where $\sin(V, V') := \|VV^\top - V'(V')^\top\|_2$. \blacksquare

It can be shown that

$$\|VV^\top - V'(V')^\top\|_2 \geq \frac{\sqrt{2}}{2} \inf_{O \in \mathbb{O}_j} \|V - V'O\|_2,$$

where \mathbb{O}_j denotes the set consisting of orthogonal square matrices with dimension j . Hence we further have

$$\inf_{O \in \mathbb{O}_j} \|V - V'O\|_2 \leq 2\sqrt{2} \frac{\|B - C\|_2}{\sigma_j(B) - \sigma_{j+1}(B)},$$

which is actually used in this paper.

Lemma 12 (Proposition 13 in Klopp (2015)) *Let X be an $n \times n$ random matrix with each entry X_{ij} being independent and bounded such that $\max_{ij} |X_{ij}| \leq \sigma$. Define*

$$\sigma_1 = \max_i \sqrt{\mathbb{E} \sum_j X_{ij}^2} \quad \text{and} \quad \sigma_2 = \max_j \sqrt{\mathbb{E} \sum_i X_{ij}^2}.$$

Then, for any $\nu > 0$, there exists constant $c = c(\sigma, \nu) > 0$ such that,

$$\|X\|_2 \leq c \max(\sigma_1, \sigma_2, \sqrt{\log n}),$$

with probability larger than $1 - n^{-\nu}$.

■

Lemma 13 (Corollary 4 and Theorem 5 in Gittens and Tropp (2009)) *Suppose B is a fixed matrix, and let X be a random matrix with each entry X_{jk} being independent and bounded such that $\max_{jk}|X_{jk}| \leq \frac{D}{2}$ almost surely, for which $\mathbb{E}(X) = B$. Then for all $\delta > 0$,*

$$\|X - B\|_2 \leq (1 + \delta)\mathbb{E}\|B - X\|_2,$$

with probability larger than $1 - \exp^{-\delta^2(\mathbb{E}\|X - B\|_2)^2/4D^2}$. Further,

$$\begin{aligned} \mathbb{E}\|X - B\|_2 &\leq c \left(\max_j \left(\sum_k \text{Var}(X_{jk}) \right)^{1/2} \right. \\ &\quad \left. + \max_k \left(\sum_j \text{Var}(X_{jk}) \right)^{1/2} + \left(\sum_{jk} \mathbb{E}(X_{jk} - b_{jk})^4 \right)^{1/4} \right). \end{aligned}$$

■

References

- James Baglama and Lothar Reichel. Augmented implicitly restarted lanczos bidiagonalization methods. *SIAM Journal on Scientific Computing*, 27(1):19–42, 2005.
- Jim Baglama, Lothar Reichel, and B. W. Lewis. *irlba: Fast Truncated Singular Value Decomposition and Principal Components Analysis for Large Dense and Sparse Matrices*, 2019. URL <https://CRAN.R-project.org/package=irlba>. R package version 2.3.3.
- Daniel Boley, Gyan Ranjan, and Zhi-Li Zhang. Commute times for a directed graph using an asymmetric laplacian. *Linear Algebra and its Applications*, 435(2):224–242, 2011.
- Daniela Calvetti, Lothar Reichel, and Danny Chris Sorensen. An implicitly restarted lanczos method for large symmetric eigenvalue problems. *Electronic Transactions on Numerical Analysis*, 2(1):21, 1994.
- Herve Cardot. *Gmedian: Geometric Median, k-Median Clustering and Robust Median PCA*, 2020. URL <https://CRAN.R-project.org/package=Gmedian>. R package version 1.2.5.
- Hervé Cardot, Peggy Cénac, Pierre-André Zitt, et al. Efficient and fast estimation of the geometric median in hilbert spaces with an averaged stochastic gradient algorithm. *Bernoulli*, 19(1):18–43, 2013.
- Xiangyu Chang, Danyang Huang, and Hansheng Wang. A popularity scaled latent space model for large-scale directed social network. *Statistica Sinica*, 29:1277–1299, 2019.
- Peter Chin, Anup Rao, and Van Vu. Stochastic block model and community detection in sparse graphs: A spectral algorithm with optimal rate of recovery. In *Conference on Learning Theory*, pages 391–423, 2015.
- Fan Chung. Laplacians and the cheeger inequality for directed graphs. *Annals of Combinatorics*, 9(1):1–19, 2005.

- Kenneth L Clarkson and David P Woodruff. Low-rank approximation and regression in input sparsity time. *Journal of the ACM (JACM)*, 63(6):1–45, 2017.
- Inderjit S Dhillon. Co-clustering documents and words using bipartite spectral graph partitioning. In *Proceedings of the seventh ACM SIGKDD international conference on Knowledge discovery and data mining*, pages 269–274, 2001.
- Petros Drineas and Michael W Mahoney. Randnla: randomized numerical linear algebra. *Communications of the ACM*, 59(6):80–90, 2016.
- Petros Drineas, Michael W Mahoney, and Shan Muthukrishnan. Sampling algorithms for ℓ_2 regression and applications. In *Proceedings of the seventeenth annual ACM-SIAM symposium on Discrete algorithm*, pages 1127–1136. Society for Industrial and Applied Mathematics, 2006.
- N Benjamin Erichson, Sergey Voronin, Steven L Brunton, and J Nathan Kutz. Randomized matrix decompositions using r. *Journal of Statistical Software*, 89(1):1–48, 2019.
- Santo Fortunato. Community detection in graphs. *Physics reports*, 486(3-5):75–174, 2010.
- Chao Gao, Zongming Ma, Anderson Y Zhang, and Harrison H Zhou. Achieving optimal misclassification proportion in stochastic block models. *The Journal of Machine Learning Research*, 18(1):1980–2024, 2017.
- Alex Gittens and Joel A Tropp. Error bounds for random matrix approximation schemes. *arXiv preprint arXiv:0911.4108*, 2009.
- Anna Goldenberg, Alice X Zheng, Stephen E Fienberg, Edoardo M Airoldi, et al. A survey of statistical network models. *Foundations and Trends® in Machine Learning*, 2(2):129–233, 2010.
- Gene Golub and William Kahan. Calculating the singular values and pseudo-inverse of a matrix. *Journal of the Society for Industrial and Applied Mathematics, Series B: Numerical Analysis*, 2(2):205–224, 1965.
- GH Golub and C Reinsch. Singular value decomposition and least squares solutions. *numerische mathematik*. 1970.
- Nathan Halko, Per-Gunnar Martinsson, and Joel A Tropp. Finding structure with randomness: Probabilistic algorithms for constructing approximate matrix decompositions. *SIAM review*, 53(2):217–288, 2011.
- John A Hartigan. Direct clustering of a data matrix. *Journal of the American Statistical Association*, 67(337):123–129, 1972.
- Paul W Holland, Kathryn Blackmond Laskey, and Samuel Leinhardt. Stochastic blockmodels: First steps. *Social networks*, 5(2):109–137, 1983.
- Pengsheng Ji and Jiashun Jin. Coauthorship and citation networks for statisticians. *The Annals of Applied Statistics*, 10(4):1779–1812, 2016.

- Brian Karrer and Mark EJ Newman. Stochastic blockmodels and community structure in networks. *Physical review E*, 83(1):016107, 2011.
- Olga Klopp. Matrix completion by singular value thresholding: sharp bounds. *Electronic journal of statistics*, 9(2):2348–2369, 2015.
- Amit Kumar, Yogish Sabharwal, and Sandeep Sen. A simple linear time $(1 + \epsilon)$ -approximation algorithm for k-means clustering in any dimensions. In *Annual Symposium on Foundations of Computer Science*, volume 45, pages 454–462. IEEE COMPUTER SOCIETY PRESS, 2004.
- Jing Lei and Alessandro Rinaldo. Consistency of spectral clustering in stochastic block models. *The Annals of Statistics*, 43(1):215–237, 2015.
- Jing Lei, Kehui Chen, and Brian Lynch. Consistent community detection in multi-layer network data. *Biometrika*, 107(1):61–73, 2020.
- Jure Leskovec, Kevin J Lang, Anirban Dasgupta, and Michael W Mahoney. Community structure in large networks: Natural cluster sizes and the absence of large well-defined clusters. *Internet Mathematics*, 6(1):29–123, 2009.
- Jure Leskovec, Daniel Huttenlocher, and Jon Kleinberg. Predicting positive and negative links in online social networks. In *Proceedings of the 19th international conference on World wide web*, pages 641–650, 2010.
- Miaoqi Li and Emily L Kang. Randomized algorithms of maximum likelihood estimation with spatial autoregressive models for large-scale networks. *Statistics and Computing*, 29(5):1165–1179, 2019.
- Ping Ma, Michael W Mahoney, and Bin Yu. A statistical perspective on algorithmic leveraging. *The Journal of Machine Learning Research*, 16(1):861–911, 2015.
- Michael W Mahoney et al. Randomized algorithms for matrices and data. *Foundations and Trends® in Machine Learning*, 3(2):123–224, 2011.
- Per-Gunnar Martinsson. Randomized methods for matrix computations. *arXiv preprint arXiv:1607.01649*, 2016.
- Xiangrui Meng and Michael W Mahoney. Low-distortion subspace embeddings in input-sparsity time and applications to robust linear regression. In *Proceedings of the forty-fifth annual ACM symposium on Theory of computing*, pages 91–100, 2013.
- Jelani Nelson and Huy L Nguyễn. Osnap: Faster numerical linear algebra algorithms via sparser subspace embeddings. In *2013 IEEE 54th annual symposium on foundations of computer science*, pages 117–126. IEEE, 2013.
- Mark Newman. *Networks*. Oxford university press, 2018.
- Sean O’Rourke, Van Vu, and Ke Wang. Random perturbation of low rank matrices: Improving classical bounds. *Linear Algebra and its Applications*, 540:26–59, 2018.

- Mert Pilanci and Martin J Wainwright. Iterative hessian sketch: Fast and accurate solution approximation for constrained least-squares. *The Journal of Machine Learning Research*, 17(1):1842–1879, 2016.
- Tai Qin and Karl Rohe. Regularized spectral clustering under the degree-corrected stochastic blockmodel. In *Advances in Neural Information Processing Systems*, pages 3120–3128, 2013.
- Yixuan Qiu and Jiali Mei. *RSpectra: Solvers for Large-Scale Eigenvalue and SVD Problems*, 2019. URL <https://CRAN.R-project.org/package=RSpectra>. R package version 0.16-0.
- Garvesh Raskutti and Michael W Mahoney. A statistical perspective on randomized sketching for ordinary least-squares. *The Journal of Machine Learning Research*, 17(1):7508–7538, 2016.
- Matthew Richardson, Rakesh Agrawal, and Pedro Domingos. Trust management for the semantic web. In *International semantic Web conference*, pages 351–368. Springer, 2003.
- Karl Rohe, Sourav Chatterjee, and Bin Yu. Spectral clustering and the high-dimensional stochastic block model. *The Annals of Statistics*, 39(4):1878–1915, 2011.
- Karl Rohe, Tai Qin, and Bin Yu. Co-clustering for directed graphs: the stochastic co-blockmodel and spectral algorithm Di-Sim. *arXiv preprint arXiv:1204.2296*, 2012.
- Karl Rohe, Tai Qin, and Bin Yu. Co-clustering directed graphs to discover asymmetries and directional communities. *Proceedings of the National Academy of Sciences*, 113(45):12679–12684, 2016.
- Liangjun Su, Wuyi Wang, and Yichong Zhang. Strong consistency of spectral clustering for stochastic block models. *arXiv preprint arXiv:1710.06191*, 2017.
- Lubos Takac and Michal Zabovsky. Data analysis in public social networks. In *International scientific conference and international workshop present day trends of innovations*, volume 1, 2012.
- Ulrike Von Luxburg. A tutorial on spectral clustering. *Statistics and Computing*, 17(4):395–416, 2007.
- HaiYing Wang, Min Yang, and John Stufken. Information-based optimal subdata selection for big data linear regression. *Journal of the American Statistical Association*, 114(525):393–405, 2019.
- Shusen Wang, Alex Gittens, and Michael W Mahoney. Sketched ridge regression: Optimization perspective, statistical perspective, and model averaging. *The Journal of Machine Learning Research*, 18(1):8039–8088, 2017.
- Duncan J Watts and Steven H Strogatz. Collective dynamics of small-world networks. *nature*, 393(6684):440, 1998.

- Rafi Witten and Emmanuel Candès. Randomized algorithms for low-rank matrix factorizations: sharp performance bounds. *Algorithmica*, 72(1):264–281, 2015.
- David P Woodruff et al. Sketching as a tool for numerical linear algebra. *Foundations and Trends® in Theoretical Computer Science*, 10(1–2):1–157, 2014.
- Haishan Ye, Yujun Li, Cheng Chen, and Zhihua Zhang. Fast fisher discriminant analysis with randomized algorithms. *Pattern Recognition*, 72:82–92, 2017.
- Se-Young Yun and Alexandre Proutiere. Optimal cluster recovery in the labeled stochastic block model. In *Advances in Neural Information Processing Systems*, pages 965–973, 2016.
- Hai Zhang, Xiao Guo, and Xiangyu Chang. Randomized spectral clustering in large-scale stochastic block models. *arXiv preprint arXiv:2002.00839*, 2020.
- Zhixin Zhou and Arash A Amini. Analysis of spectral clustering algorithms for community detection: the general bipartite setting. *Journal of Machine Learning Research*, 20(47):1–47, 2019.